UNIVERSIDADE D
COIMBRA

Danielle Lacerda Rudley

Assessing alpine shrub response to climate change

Dissertação orientada pelas Professoras Doutoras Cristina Nabais e Susana Rodríguez Echeverría no âmbito do Mestrado de Ecologia do Departamento de Ciências da Vida, Faculdade de Ciências e Tecnologia, Universidade de Coimbra.

Outubro de 2020

Departamento de Ciências da Vida
Faculdade de Ciências e Tecnologia
Universidade de Coimbra

Assessing alpine shrub response to climate change

Danielle Lacerda Rudley

Dissertação orientada pelas Professoras Doutoras Cristina Nabais e Susana Rodríguez Echeverría no âmbito do Mestrado de Ecologia do Departamento de Ciências da Vida, Faculdade de Ciências e Tecnologia, Universidade de Coimbra.

Trabalho realizado no âmbito do projeto de investigação "Estrela - Effect of global warming on the diversity and functioning of the alpine ecosystems of Serra da Estrela, a threatened mountain range in the transition area between temperate and Mediterranean climates" com referência PTDC/BIA-CBI/30215/2017 (CENTRO-01-0145-FEDER-030215), co-financiado pelo Fundo Europeu de Desenvolvimento Regional (FEDER), através do programa Portugal-2020 (PT2020), no âmbito do Programa Operacional Regional do Centro e pela FCT/MCTES através de fundos nacionais (PIDDAC). Este trabalho foi realizado na Unidade de I&D Centre for Functional Ecology – Science for People & the Planet (CFE), com a referência UIDB/04004/2020, com apoio financeiro da FCT/MCTES através de fundos nacionais (PIDDAC).

ABSTRACT

Serra da Estrela is an exceptional place to study the effect of global warming on ecosystems since it is in the transition zone between the Mediterranean and temperate climates. Serra da Estrela is also the highest mountain range and only alpine region in continental Portugal, thus, having a huge interest for conservation. However, thus far, there is little research on the response of Estrela alpine ecosystems to global warming.

We used dendrochronological and quantitative wood anatomy techniques to analyze the response to climate of the two main alpine shrub species of Serra de Estrela, *Juniperus communis* subsp. *alpina* and *Cytisus oromediterraneus*. Our main hypotheses were 1) Shrub growth has increased for both species in the last 5 years following the current warming trend; 2) SRW will be positively influenced by increases in temperature in spring and autumn, i.e., at the beginning and end of the growing season; and 3) wood anatomy is more affected by precipitation in *C. oromediterraneus* than in *J. communis*.
Shrub ring width displayed a positive trend from 2015-2019, coinciding with an increasing trend in global temperatures. Generalized Additive Models indicated spring and autumn temperatures influenced *J. communis* SRW, and spring and autumn precipitation most influenced *C. oromediterraneus* SRW. Thus, a longer growth period due to warming has a direct effect only for *J. communis* subsp. *alpina*. In addition, *J. communis* hydraulic conductivity was influenced by early spring and autumn precipitation, while spring and summer temperature did so for *C. oromediterraneus*.

These results indicate that warming can promote the growth of the two dominant alpine shrub species in the high plateau of Serra da Estrela Natural Park, but may eventually lead to changes in plant performance and distribution shifts in the longer term due to species-specific differences in the response to climatic variables.

Keywords: Dendrochronology, Wood anatomy, Global warming, Alpine shrubs, Hydraulic conductivity

RESUMO

A Serra da Estrela encontra-se na zona de transição entre o clima mediterrâneo e temperado, constituindo um local excecional para estudar o efeito do aquecimento global nos ecossistemas. É também a cordilheira mais alta e única região alpina de Portugal continental, com um elevado interesse para a conservação. No entanto, ainda há poucos estudos sobre a resposta deste ecossistema ao aquecimento global.

Com base em dados dendrocronológicos e de anatomia quantitativa do xilema, analisou-se a resposta ao clima das duas principais espécies de arbustos alpinos da Serra da Estrela, *Juniperus communis* subsp. *alpina* e *Cytisus oromediterraneus*. As hipóteses principais foram 1) O crescimento das duas espécies aumentou nos últimos 5 anos seguindo a tendência de aquecimento; 2) A largura do anel apresenta uma correlação positiva com a temperatura na primavera e outono; e 3) a anatomia da madeira é mais afetada pela precipitação em *C. oromediterraneus* do que em *J. communis*.

A largura do anel apresentou uma tendência positiva de 2015-2019, coincidindo com o aumento das temperaturas globais. Modelos aditivos generalizados indicaram que o crescimento de *J. communis* foi influenciado pelas temperaturas de primavera e outono, enquanto *C. oromediterraneus* foi mais afetado pela precipitação de primavera e outono. Isto indica que o aumento da estação de crescimento devido ao incremento da temperatura terá um impacto maior no crescimento de *J. communis*. Adicionalmente, a condutividade hidráulica de *J. communis* foi influenciada pela precipitação do início da primavera e outono, enquanto que em *C. oromediterraneus* o mesmo parâmetro foi afetado pela temperatura da primavera e do verão.

Estes resultados indicam que o aquecimento pode promover o crescimento das duas espécies dominantes de arbustos alpinos no planalto da Serra da Estrela, mas pode eventualmente resultar em alterações na distribuição a longo prazo devido a diferenças específicas das espécies em resposta às variáveis climáticas.

Palavras-chave: Dendrocronologia, Anatomia da madeira, Aquecimento global, Arbustos alpinos, Condutividade hidráulica

ACKNOWLEDGEMENTS

Firstly, I would like to thank my parents. You've always told me to follow my dreams and ambitions and believed in me even in times when I didn't believe in myself. And although it has been so hard to be separated from you by an ocean, love crosses all bounds and I am so grateful for your support.

I never would have discovered the opportunity to gain this enriching experience if it weren't for my cousin Allana. You are more of a sister than a cousin, and your guidance and emotional support was paramount for me to not only successfully pursue a graduate degree after being away from academia for so long, but also make a new home and life in a foreign country.

I would like to thank Alexandre from CISE for his help conducting fieldwork and teaching me about Serra da Estrela. You are a bottomless well of knowledge, and the only person I know with bad eyesight who can find a tiny, rare flower in the middle of the mountains.

I feel so incredibly lucky to have had Cristina and Susana as my supervisors and mentors. I learned how to be a better writer and scientist by working with you, and I hold you both in very high regard. You are amazing women in science, I hope to follow suit and look forward to working with you in the future.

Ana Luísa Carvalho. Where do I begin? This thesis would never have come to fruition if it weren't for you. The quality of my technical work is because of your training in the lab. My Portuguese is only at the level that it is because of your unending patience. And you always knew when to remind me to manage my stress and practice self-care. Throughout this thesis you were an anchor for me and undoubtedly, I am a better researcher and a better person for having met you.

Lastly, and very especially, I would like to thank my partner Tocayo. Thank you for always pushing me to grow and helping me maintain perspective. This experience was a rollercoaster of emotions, and I'm so glad you were by my side for this ride.

TABLE OF CONTENTS

LIST OF FIGURES

LIST OF TABLES

LIST OF EQUATIONS

LIST OF ABBREVIATIONS

ALA – Average Lumen Area

AOGCMs – Atmosphere-Ocean General Circulation Models

ANOVA – Analysis of Variance

AP – Axial Parenchyma

BRW – Branch Ring With

COB – Covão do Boi

EW – Earlywood

F – Fiber

GAMs – Generalized Additive Models

H_D – Hydraulic Diameter

IPMA – Instituto Português do Mar e da Atmosfera

K_H – Hydraulic Conductivity

LW – Latewood

MLA – Maximum Lumen Area

N – Number of conduits

NSA – Nave de Santo António

PEG – Penha do Gato

PNSE – Parque Natural da Serra de Estrela

R_L – Lumen Resistivity

RP – Ray Parenchyma

SRW – Shrub Ring Width

TE – Tracheary Element

VE – Vessel Element

VT – Vascular Tracheid

INTRODUCTION

A. CLIMATE CHANGE

Climate change is mainly associated with the current global rise in temperature and the related consequences such as increases in the frequency and severity of extreme weather phenomena, and changes in disturbance regimes (Carnicer et al., 2011; Gazol et al., 2018; Peña-Gallardo et al., 2018; Yin & Bauerle, 2017). According to the latest Global Climate Report (2019) from the National Oceanic and Atmospheric Administration, the last five years have presented the five highest temperature anomalies on record (figure 1).

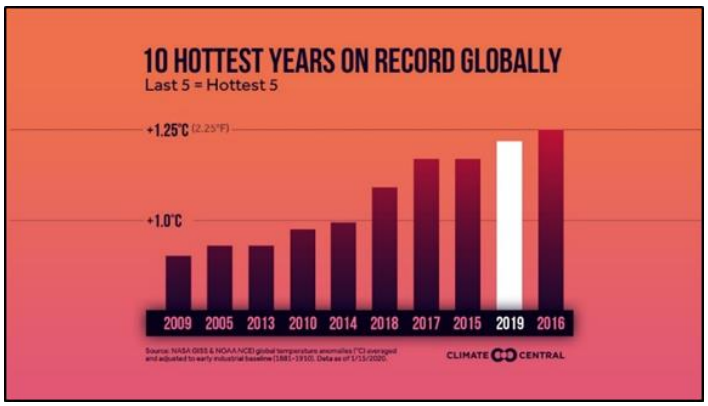

Figure 1. Top 10 years with the highest temperature anomalies. The top 5 years with the highest temperatures were between 2015-2019. Source: climatecentral.org

Global temperatures are expected to increase between 1.5 - 4ºC by the end of this century (Anadon-Rosell et al., 2014; Rustad et al., 2001), likely resulting in significant shifts in climate patterns. It is also evident that increases in global temperatures will result in an increase of the frequency and severity of drought events, as it has already been observed in the Mediterranean (Gazol et al., 2018; Vieira et al., 2020). Indeed, several Atmosphere-Ocean General Circulation Models (AOGCMs) predict future warmer climates with drier summers and an increased risk of drought in characteristically arid regions such as the Mediterranean as well as middle and high latitudes in the northern hemisphere (Meehl et al., 2007; Copenheaver et al., 2010).

Global warming affects the growth, physiology, fitness and distribution of plants (Chapin et al., 2005; Lu et al., 2019; Sturm, 2005; Thuiller et al., 2005) through numerous direct and indirect effects. However, the outcome of these changes may be difficult to predict as there may be multiple, interconnected driving factors affecting different ecosystem processes (Kudo & Suzuki, 2003; Rustad et al., 2001). In addition, these effects may elicit different responses among co-occurring species which could potentially establish climate feedback loops due to changes in species composition and cover, further altering the mosaic of plant species communities (Anadon-Rosell et al., 2014; Garcia-Cervigón et al., 2012; Gazol et al., 2018; Peña-Gallardo et al., 2018).

The impact of global warming on terrestrial ecosystems has been forecasted to be greatest in mountain and arctic regions (Anadon-Rosell et al., 2014; Bär et al., 2006). Climate conditions in mountainous regions change with elevation (Midolo et al., 2019), leading to a distribution of

plant communities in a gradient associated with altitudinal belts (Elsen et al., 2018), transitioning from forest, shrubland, and alpine grassland up to the nival zone with a permanent snow cover. Altitudinal belts are characterized by soil composition, geographic location and topography, but mainly by isotherms and precipitation (Frahm & Gradstein, 1991). In the alpine zone, above the tree line, plant growth is constrained by a harsh environment characterized by low minimum temperatures, strong winds, short growing seasons and frequent freezing events that occur outside of the winter season (Anadon-Rosell et al., 2014). In Mediterranean mountains these growth constraints are further exacerbated by greater fluctuations of seasonal temperatures and precipitation, as well as summer drought conditions characteristic to the region (Anadon-Rosell et al., 2014; Camarero et al., 2010; Garcia-Cervigón et al., 2012; Olano et al., 2013).

Increasing temperatures in mountains have promoted the migration of plant species upwards, following their optimal climatic conditions (Pauli et al., 2012; Theurillat & Guisan, 2001), and resulting in significant shifts in species distribution (Díaz-Varela et al., 2010). However, the species' ability to migrate at a rate comparable to the rate of temperature increase appears to be species-specific, and is also likely to play a role in plant communities composition under warming conditions (Kudo & Suzuki, 2003). A common phenomena observed in alpine zones as a result of warming is the expansion of shrublands or shrub encroachment (Sanz-Elorza, 2003). There are important differences on the effect of warming in alpine plant diversity in Temperate and Mediterranean mountains. These shifts had opposite effects on the summit floras' species richness in boreal-temperate mountain regions (+3.9 species on average) and Mediterranean mountain regions (–1.4 species), probably because recent climatic trends have decreased the availability of water in the Mediterranean (Pauli et al., 2012; Thuiller et al., 2005).

Climatic models predict a temperature rise in mountainous regions, an aridity increase in drought-prone areas from the Circum-Mediterranean region, and an estimated decrease of 11-17% of total annual precipitation in the Mediterranean (Christensen et al., 2007; Vieira et al., 2020) therefore, understanding how shrubs respond to such climatic oscillations might be of primary interest for the conservation of these communities (Gazol et al., 2018). It is also important to note that drought legacy effects, which affect a plant's ability to recover from a drought event, are positively correlated with aridity (Kannenberg et al., 2019) and therefore, increases in drought events are highly likely to have a pronounced negative impact on plant growth in Mediterranean regions.

B. SERRA DA ESTRELA

Geography and climate

Figure 2. Central Iberian System. Source: Nations Online Project

The Serra da Estrela, henceforth referred to as Estrela, is the westernmost mountain range of the Central Iberian System (fig. 2) and biogeographically located in the Estrelensean sector within the Carpetanian-Leonese Subprovince (Meireles et al., 2013; Mora, 2010). This granitic plateau is the highest point in mainland Portugal, reaching an elevation of 1,993m (fig. 3). Estrela is in the transition between Mediterranean and temperate climates (Meireles et al., 2012), and therefore, an area where species turnover is expected to be especially high in response to climate change (Thuiller et al., 2005). This massif is dominated by siliceous substrates, mainly granite and schist, and is a landscape marked by the last major glaciation (Meireles et al., 2013; Mora, 2010; Van Der Knaap & Van Leeuwen, 1997). Its proximity to the coast (<100km) results in an oceanic influence than can be detected at higher elevations (Meireles et al., 2009), and the topography and geographic location of Estrela creates distinct and unique conditions optimal to promote the formation of microclimates and a high rate of endemism (Meireles et al., 2013; Mora, 2010).

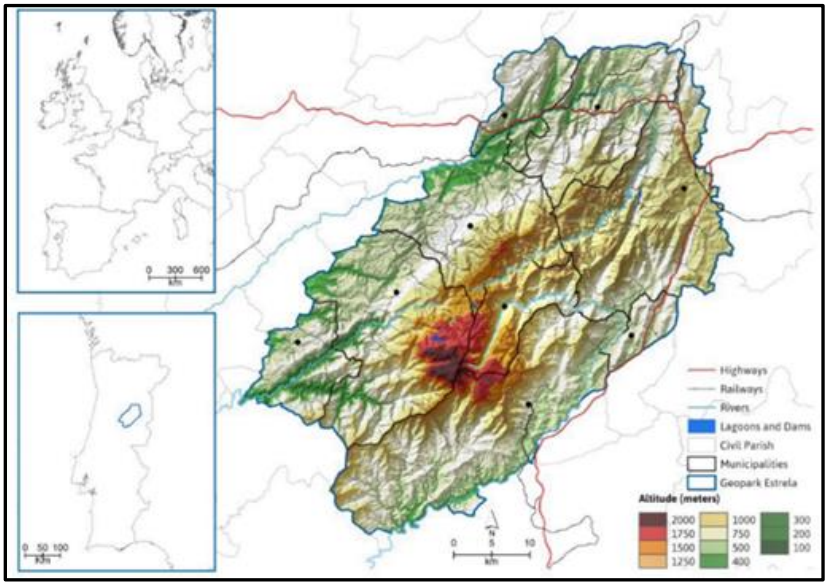

Figure 3. Map of Serra da Estrela Natural Park (PNSE). Source: GeoPark Estrela

In a broader sense, three distinct bioclimatic belts can be distinguished in Serra de Estrela: lower (up to 800m), intermediate (800-1600m) and upper (1600-1993m) belts (Jansen, 2011) (fig. 4). The lower and intermediate belts have been heavily exploited by humans and as a result, the climax vegetation of *Quercus* forests is very rare (Jansen, 2011). These forests

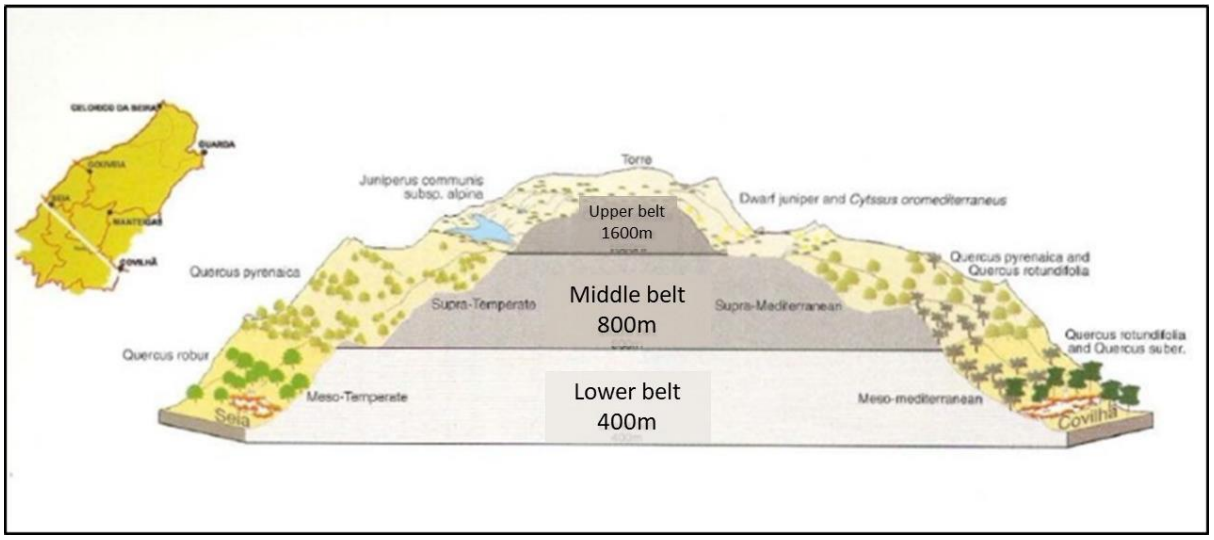

Figure 4. Bioclimatic belts of Serra da Estrela. Source: Jansen 2002

have been replaced mainly by agriculture land, pasturelands and shrublands, with an increasing presence of invasive plant species. The upper belt contains the alpine zone characterized by the absence of trees and the presence of alpine shrublands and grasslands. This upper belt contains the less disturbed areas with habitats of high priority for conservation which are currently threatened by global warming.

Alpine shrublands are particularly widespread and important in the upper belt of Estrela due to the provision of multiple ecosystem services including regulation of the water cycle, carbon storage, biodiversity conservation and the provision of important habitat and food sources for other organisms. In the higher elevation, Estrela alpine shrublands are dominated by dwarf juniper formations of *Juniperus communis* subsp. *alpina* (Suter) Celak. (hereafter *J. communis*), and legume shrublands of *Cytisus oromediterraneus* Rivas Mart. et al (hereafter *C. oromediterraneus*).

J. communis heaths are the dominant basal communities in the Oro-Mediterranean and Sub-Mediterranean Oro-Temperate climates within Estrela (Meireles et al., 2009). Although studies suggest that thermophilous heaths such as the *J. communis* heaths found in Estrela are better adapted to warming than their mesophilous counterparts (Theurillat & Guisan, 2001), García et al. (1999) found that *J. communis* seedling survival is lower in driers sites than more humid sites, which may play a crucial role in post-disturbance succession and establishment.

C. oromediterraneus formations are common matorrals in humid, high elevation zones of Mediterranean mountains with acidic soils, and may be indicative of climax vegetation (Fernández-Santos et al., 2004; Jansen, 2011; ICNF 2006). In Estrela these matorrals are often associated with the presence of *J. communis* however, while *J. communis* heaths are common throughout the alpine and sub-alpine region of Estrela, *C. oromediterraneus*

formations mainly occur in the southeast portion of the mountain range; Jansen (2011) infers that this dichotomy illustrates the transition from Mediterranean to Temperature influence in the region.

J. communis and *C. oromediterraneus* shrubs may have very different effects on soil communities and C and N cycling due to specific litter quality and differential association with soil mutualists (Montané et al., 2007). Thus, understanding the response of both species to global warming might give us an indication of the consequences of climate change for the functioning of alpine ecosystems in Serra da Estrela.

C. DENDROCHRONOLOGY

Woody growth rings are developed by the seasonal activity of the vascular cambium, with ring boundaries indicating the period of dormancy (Schweingruber et al., 2013) and are composed of xylem tissue used for conducting water throughout the plant, and for the mechanical strength of the stem. Dendrochronology is the scientific method of dating growth rings in woody species (Tenzin & Dukpa, 2017). Dating wood rings is based on crossdating growth patterns of different individuals from the same area, assuming that climatic conditions will have a strong impact on the interannual growth variations (Chan et al., 2013). Crossdating ensures that individual wood rings are being correctly identified. Larger growth rings indicate the capacity for more water conduction, due to either larger or more xylem cells, and infer a more favorable growth year, while smaller rings indicate unfavorable growth years (fig.5) (Lovisolo & Schubert, 1998; Scholz et al., 2013).

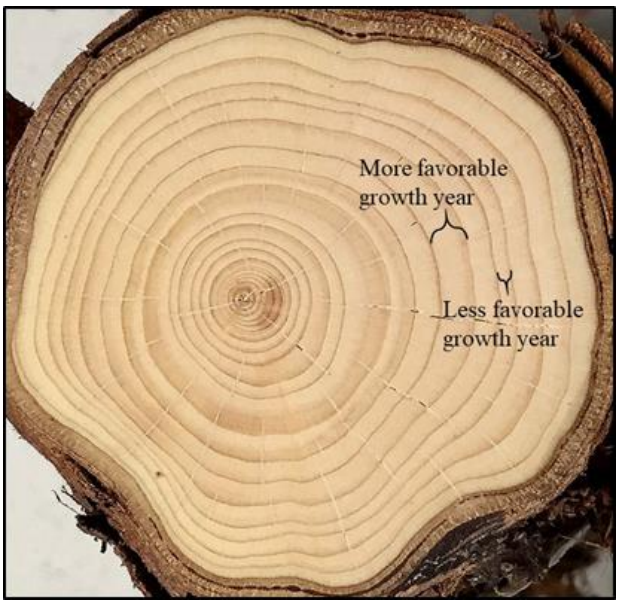

Figure 5. Growth rings of Juniperus communis subsp. alpina.

The information derived from dendrochronological analyses can be utilized to help reconstruct past climates, as well as to infer plant growth sensitivity to changes in climatic conditions and plant response to environmental stressors (Gazol et al., 2018; Myers-Smith et al., 2015; Peña-Gallardo et al., 2018). Indeed, one of the best ways to predict future vegetation shifts in response to climate change is to examine historical responses of existing plants through dendroecological methods (Copenheaver et al., 2010).

Dendrochronological techniques have been extensively used for studies in regions with water limitation, such as those under Mediterranean climate, to analyze cambial activity in drought conditions (Vieira et al., 2013, 2020). While dendrochronological and dendroecological studies in the Mediterranean have mainly focused on tree species (Garcia-Forner et al., 2019; Vieira et al., 2015; Abrantes et al., 2012; Camarero et al., 2010) the use of shrubs species has recently gained attention since they can provide information from habitats heavily threatened by warming where there are none or few trees (Bär et al., 2006). The information obtained from Mediterranean alpine shrub growth rings could allow us to gain further insight into past climatic conditions at elevations above the tree line and better understand the effects of climate change on vegetation in these regions (Bär et al., 2008; Garcia-Cervigón et al., 2012; Myers-Smith et al., 2015; Zimowski et al., 2014).

D. PLANT GROWTH

Wood can be classified as one of two types: softwood (gymnosperms) and hardwood (angiosperms). Softwood is constituted by tracheids (fig. 6), which are long, overlapping cells with tapered ends and pits arranged in either an opposite or alternate pattern (Butterfield & Meylan, 1980). Tracheids are an evolutionarily simpler vascular tissue, compared to vessel elements of the angiosperms, and serve a dual function of water conduction and mechanical support (Sperry et al., 2006). Gymnosperms also contain ray and a small amount of axial parenchyma which transport sugars laterally and axially throughout the plant, respectively (fig 6). Parenchyma abundance, and proximity to tracheary elements, may also help minimize embolism damage via outgrowths called tyloses (Olano et al., 2013; Schirarend, 2008; Sperry et al., 2006). In line with this, some studies suggest that parenchyma abundance may be influenced by climate (Butterfield & Meylan, 1980; Olano et al., 2013).

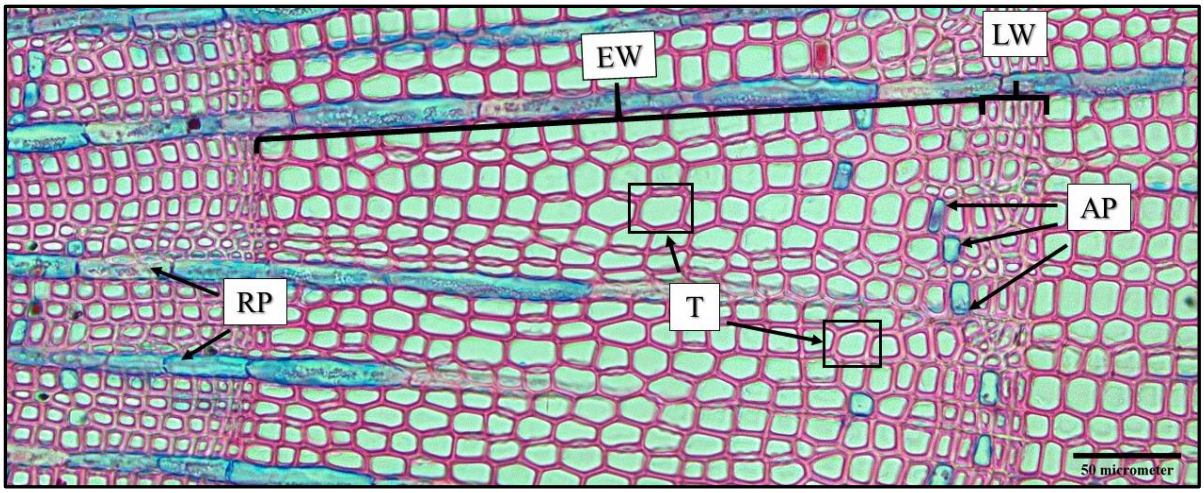

Figure 6. Softwood cross section of Juniperus communis subsp. alpina. AP – axial parenchyma; EW – early wood; LW – latewood; RP – ray parenchyma; TE – tracheary element.

Hardwood conducts water via vessel elements (fig. 7) which may vary in size, density and arrangement (Rodriguez-Zaccardo et al., 2019), and has libriform fibers for mechanical support (fig. 7). Vessel elements, hereafter referred to as vessels, are generally shorter and wider than tracheids and connect end-to-end via perforation plates, allowing for easy transport of water. Several species of angiosperms also contain vascular tracheids, which are non-perforate like true tracheids, but contain large bordered pits similar to those found in vessels (fig. 7). Vascular tracheids usually only occur during latewood, at the end of the growth ring, and function as supplementary water conductors to adjacent vessels. Once latewood has completed formation vascular tracheids may also function in support (Carlquist, 1985).

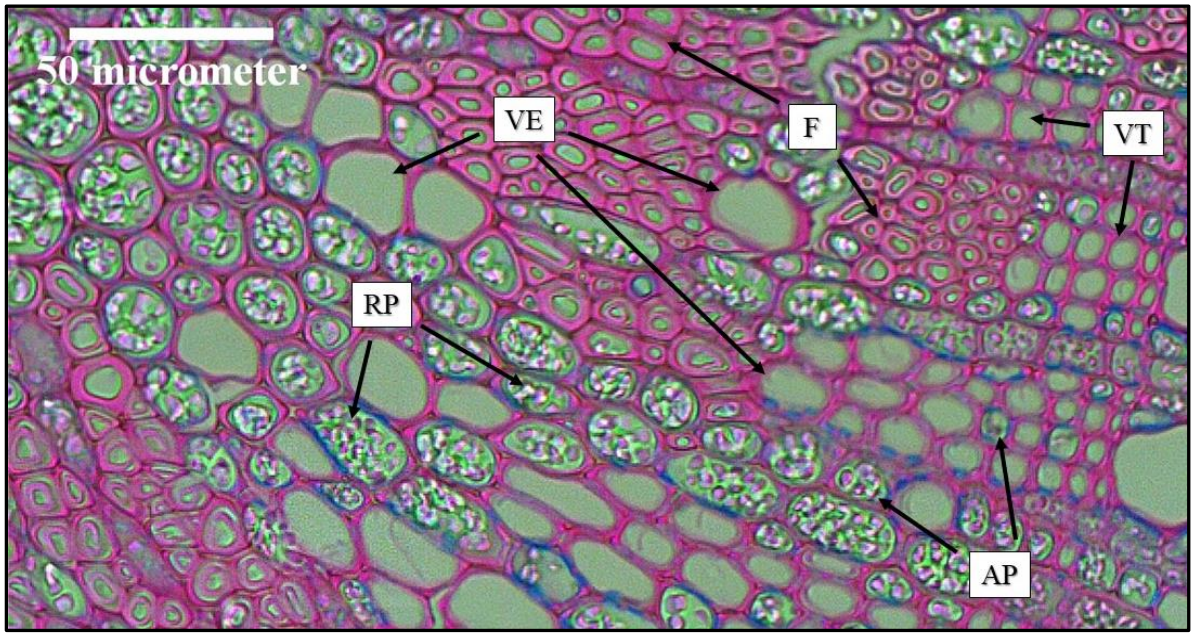

Figure 7. Hardwood cross section of Cytisus oromediterraneus. AP – axial parenchyma; F – fiber; RP – ray parenchyma; VT– vascular tracheid; VE – Vessel element.

Plant water conduction begins at the leaf where tension is generated in the tracheary elements via evapotranspiration at the leaf surface, creating a negative pressure between the vapor pressure inside the xylem cell and the pressure of the xylem cell itself. This causes water absorbed by the roots to ascend through the tracheary elements, transporting water throughout the plant body to the leaves (Olson et al., 2014, 2018; Tyree, 1997). Plant hydraulic conductivity, which reflects the water conducting capacity of these tracheary elements, is directly related to vessel lumen diameter; vessels with larger diameters have the potential to transport more water throughout the plant (Scholz et al., 2013; Sperry et al., 2005). However, there is a trade-off between efficiency and safety (Vieira et al., 2014). While larger conduits may transport greater quantities of water, they must also maintain the state of tension based on the levels of evapotranspiration occurring on the leaf surface. If there is not sufficient water available to maintain this metastable state then embolisms, or air bubbles, are likely to form,

which disrupt the water column and may limit growth; cases where embolisms are abundant may even result in plant death (Ogasa et al., 2013; Pittermann & Sperry, 2003; Sperry & Sullivan, 1992). Conditions such as extremely low temperatures or low water availability significantly increase the likelihood of embolism development (Charrier et al., 2014). In addition, tracheary elements are more likely to develop embolisms from freezing and thawing at diameters greater than 30µm (Sperry et al., 2006). Thus, plants in drier and colder climates will tend to develop narrower, more slowly conducting tracheary elements (Lovisolo & Schubert, 1998; Olano et al., 2013; Olson et al., 2014, 2018). Studies also suggest that plants in harsh environments are likely to have a higher abundance of paratracheal parenchyma to refill xylem cavities and mitigate damage from embolisms (Olano et al., 2013).

Studies have shown that temperature and water availability influence wood formation (Garcia-Cervigón et al., 2012; Garcia-Forner et al., 2019; Vieira et al., 2014; Zimowski et al., 2014), and wood anatomical characteristics are indicative of plant response to environmental stressors such as increasing temperatures and severe drought events. Literature regarding the effects of drought among wood types suggests that anatomy has a significant influence on legacy effect size (Kannenberg et al., 2019). For example, gymnosperms can survive in cold, dry, growth-limiting conditions and are less susceptible to water stress compared to angiosperms. *J.* communis, specifically, has shown drought tolerant behavior (Zweifel et al., 2009; Thomas et al., 2007). However, angiosperms appear to have less drought legacy effects than gymnosperms and therefore, less difficulty in post-drought recovery of hydraulic conductivity (Anderegg et al., 2015; Camarero et al., 2010; Kannenberg et al., 2019; Sperry et al., 2006). This supports findings from Ogasa et al. (2013) that suggest a tradeoff between resilience to drought and post-drought recovery in angiosperms. Although there may be differing responses between species to decreasing water availability, one thing is clear: the effects of drought negatively impact plant growth across biomes (Yin & Bauerle, 2017).

OBJECTIVES AND HYPOTHESES

This study was conducted as part of the project “Estrela - Effect of global warming on the diversity and functioning of the alpine ecosystems of Serra da Estrela, a threatened mountain range in the transition area between temperate and Mediterranean climates” (PTDC/BIA-CBI/30215/2017). There has been a clear increase in average, minimum and maximum temperatures in Estrela over the last thirty years (fig. 8), with unknown effects on the alpine plant communities. Therefore, it is crucial to understand plant growth in response to changes in temperature and precipitation, especially in areas particularly vulnerable to the effects of climate change such as the high plateau of Serra da Estrela.

This thesis aims to analyze growth rings and wood anatomy of the two main alpine shrubs in Serra da Estrela, *Juniperus communis* subsp. *alpina* and *Cytisus oromediterraneus,* to understand the effect of temperature and precipitation in shrub secondary growth. Our main hypotheses are:

1. Shrub growth has increased for both species in the last 5 years following the current warming trend, since increasing temperatures have a positive effect on alpine shrub growth (Anadon-Rosell et al., 2014).
2. Warming may increase alpine plant growth due to an extension of the growing season (Peñuelas & Filella, 2001). Thus, SRW will be positively influenced by increases in temperature in spring and autumn, i.e., at the beginning and end of the growing season.
3. Gymnosperms are expected to be more resistant to drought than angiosperms due to the specificities of their wood anatomy (Zweifel et al., 2009), thus, we expect wood anatomical and hydraulic parameters to be more affected by precipitation in *C. oromediterraneus* than in *J. communis*.

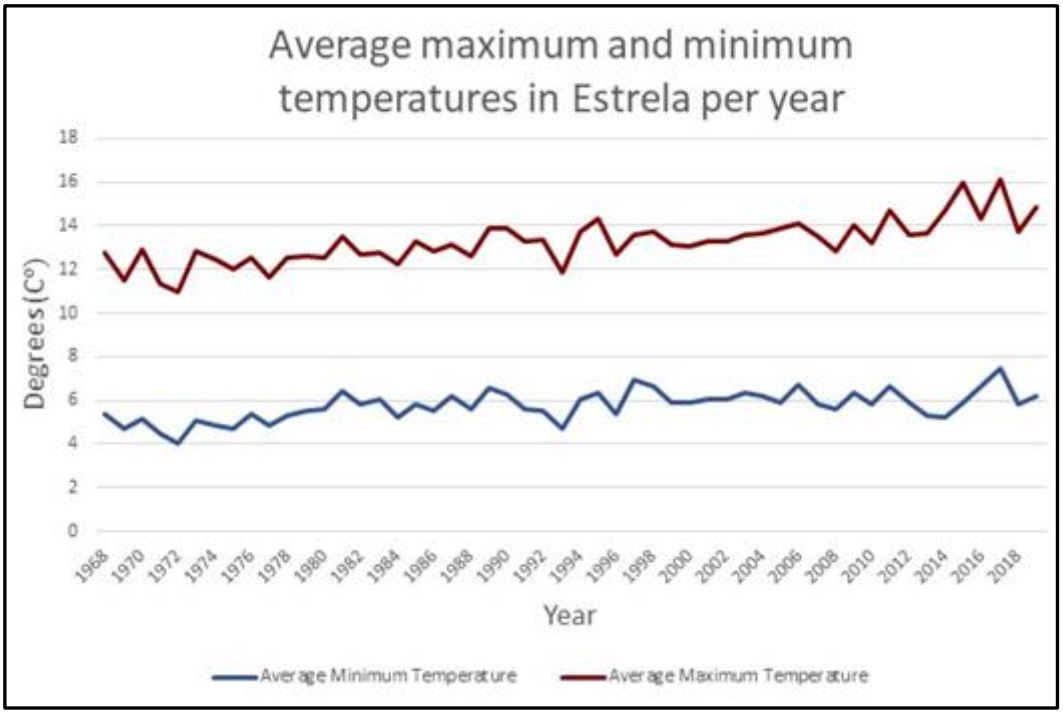

Figure 8. Temporal trends (1968-2019) for maximum and minimum temperatures in Serra da Estrela. Source: IPMA

MATERIALS & METHODS

A. STUDY SITE AND SAMPLING

1. Study site

Sampling was conducted in three shrublands dominated by either *J. communis* or *C. oromediterraneus* within the alpine vegetation belt of the Serra da Estrela, between the altitudes of 1563-1872m. Samples were collected at the end of the growing season in late October. The three sampled sites were located, from the highest elevation to the lowest elevation, in Covão do Boi (COB), Penha do Gato (PEG), and in Nave de Santo António (NSA) (fig. 9). Altitude, orientation, and slope were measured in all sampling sites. Since all samples were collected on a plateau slope was 0, and thus, this parameter was excluded from statistical analysis.

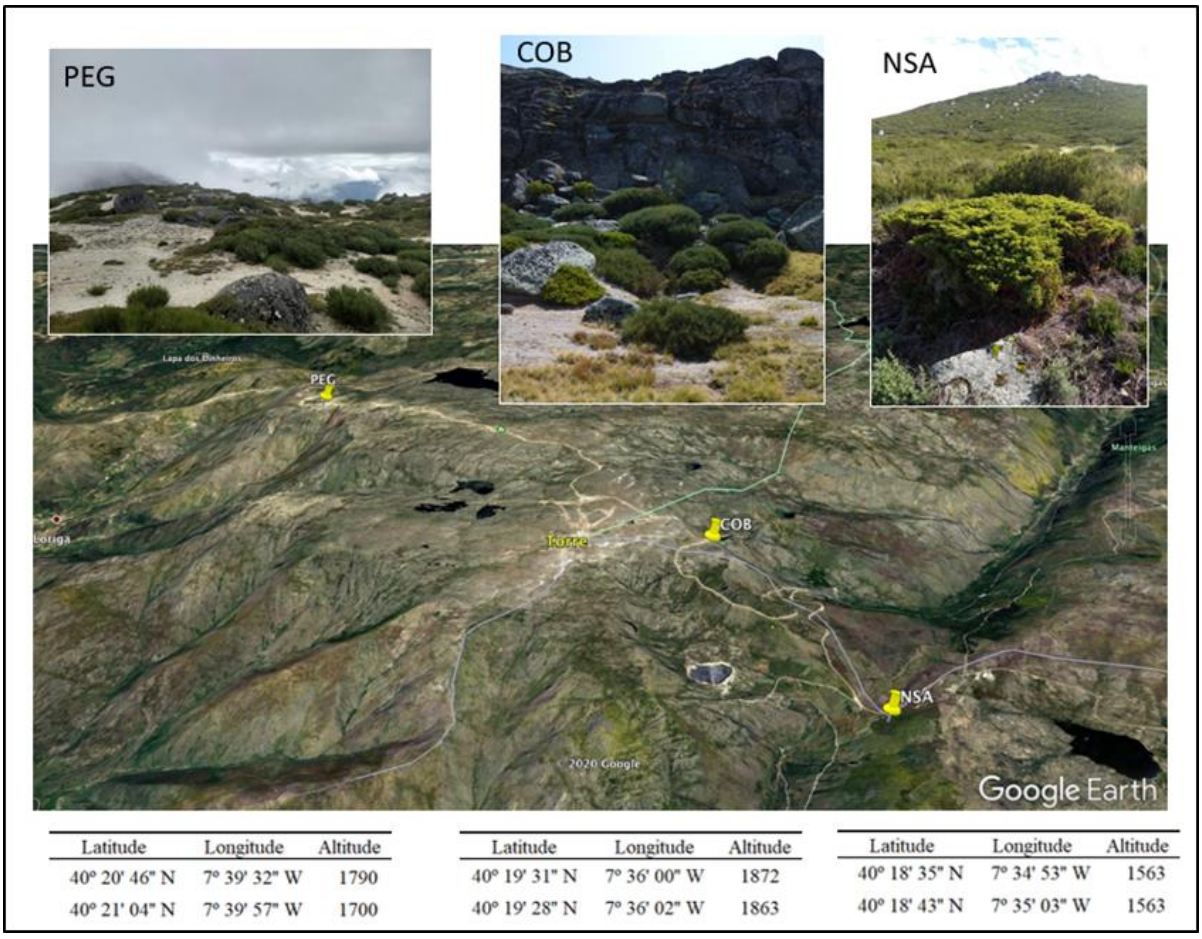

Latitude	Longitude	Altitude
40º 20' 46" N	7º 39' 32" W	1790
40º 21' 04" N	7º 39' 57" W	1700

Latitude	Longitude	Altitude
40º 19' 31" N	7º 36' 00" W	1872
40º 19' 28" N	7º 36' 02" W	1863

Latitude	Longitude	Altitude
40º 18' 35" N	7º 34' 53" W	1563
40º 18' 43" N	7º 35' 03" W	1563

Figure 9: Sampling sites within the alpine zone of PNSE from west to east: Penha do Gato (PEG), Covão do Boi (COB), and Nave do Santo Antonio (NSA).

Samples from COB were collected in the transition between a rocky outcrop and grasslands. Vegetation was arranged in a mosaic of open shrub stands with the presence of *J. communis, C. oromediterraneus, Erica* spp. and *Calluna vulgaris* as well as the presence of grassland

flora such as *Nardus stricta, Festuca henriquesii, Galium saxatile* var. *vivanium* and *Campanula herminii*. PEG was located in a habitat with rockier soil and more sparse vegetation, composed of open stands of *J. communis, C. oromediterraneus* and *Erica* spp.shrubs. Samples from NSA were collected in the transition zone between dense shrubland and grassland; woody species present included *J. communis, C. oromediterraneus, Calluna vulgaris, Genista anglica,* and *Erica* spp.

Minimum, maximum and average monthly temperatures as well as monthly total precipitation were obtained from Penhas Douradas observatory (IPMA), located 1380 masl, from the years 1968-2019.

2. *Study species*

J. communis and *C. oromediterraneus,* the two dominant shrub species in the alpine vegetation belt in Serra da Estrela, were selected for this study. Both have a small distribution in Portugal, that is almost restricted to the upper plateau in Serra da Estrela and, thus, are vulnerable to changes in this habitat (fig. 10).

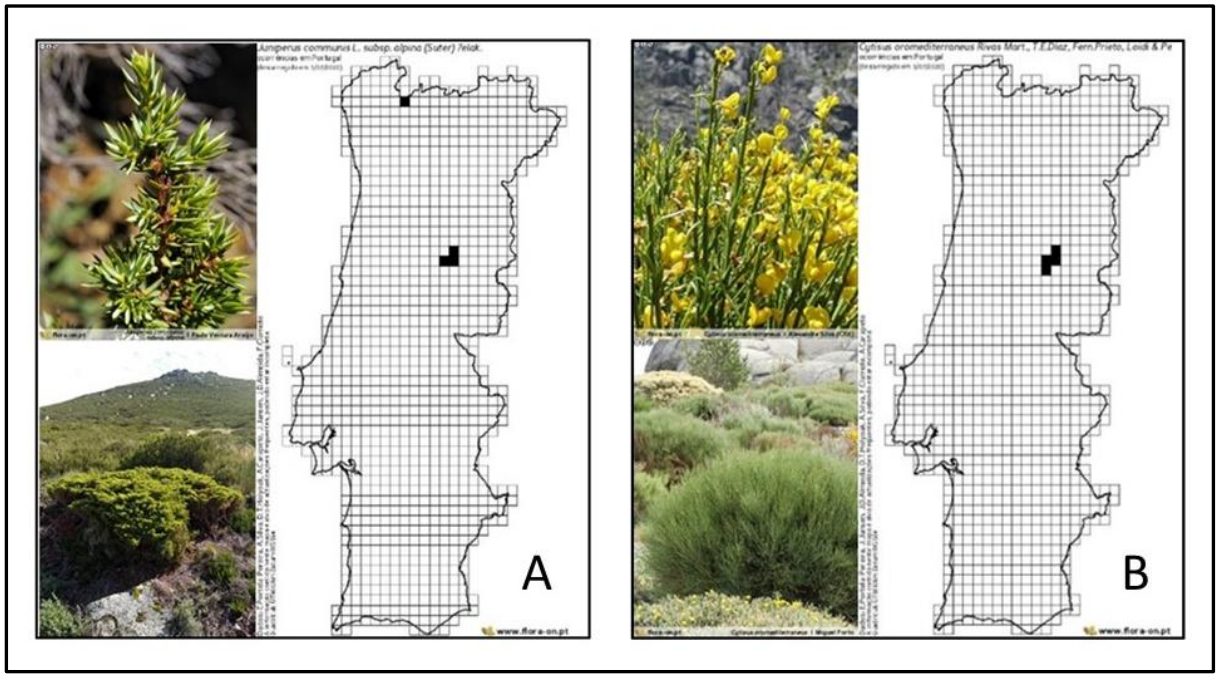

Figure 10. Distribution of Juniperus communis L. subsp. alpina (Suter) Celak (A) and Cytisus oromediterraneus Rivas-Martínez (B) in Continental Portugal. Source: Flora-on.pt

2.1. *Juniperus communis* L. subsp*. alpina* (Suter) Celak

J. communis is a coniferous, dioecious shrub that grows up to 50cm in height and 3m in diameter (fig. 10A). *J. communis* is a heliophilic, drought tolerant species (Thomas et al., 2007) that is extremely prevalent in the high mountains of central and southern Europe and, depending on local conditions, may form either dense stands or patches in a scrubland/grassland mosaic (Jansen, 2011; Schweingruber et al., 2013; European Red List of Habitats, 2016). Although commonly found in Estrela at elevations above 1,600 masl, it is one of only two occurrences of *J. communis* in continental Portugal, the other being Serra do Gerês (Costa et al., 1998). Harsh conditions common to the Mediterranean alpine vegetation belt influence the phenology of this species, resulting in procumbent nanophanerophytes who are likely to have small ring widths, stem lobes and the frequent presence of growth anomalies such as false and locally absent rings (Bergmeier et al., 2014; Garcia-Cervigón et al., 2012; Myers-Smith et al., 2015; Schweingruber et al., 2013). *J. communis* species prefer moister climates (Thomas et al., 2007), and in high elevation Mediterranean regions appear to have a strong climatic signal with precipitation during the growing season, and a positive correlation between radial growth and spring temperatures (Garcia-Cervigón et al., 2012).

2.2 *Cytisus oromediterraneus* Rivas-Martínez

C. oromediterraneus is a shrubby legume that may reach up to 100 cm (fig. 10B) and is endemic to southern Europe; its only occurrence in Portugal is in Estrela (Jansen, 2011). This phanerophyte is primarily found in elevations above 1,400m, and can be found growing on granitic slopes or forming dense stands in acidic soils (Meireles et al., 2013; Fernández-Santos et al., 2004). This species may be present in harsh environments, even in conditions of low water availability (Meireles et al., 2013). *C. oromediterraneus* occurs in the transition zone between Mediterranean and Eurosiberian climates and, due to its unique habitat and limited distribution, can serve as a bioindicator of climate change on a local or regional level (Meireles et al., 2013).

It is also interesting to note that *C. oromediterraneus* exhibits a resilience to fire disturbance in part through its below-ground morphology, and flourishes in habitats subject to fire disturbance as well as traditional pastoralism practices (Fernández-Santos et al., 2004; Meireles et al., 2013; ICNF, 2006).

3. Sampling design

Eight individuals of both *J. communis* and *C. oromediterraneus* were selected from each of the three sites for a total of 24 individuals per species. Shrub height and diameter were measured for each shrub sampled. From each individual, three branches were selected and cut at a distance of 20 cm from the apical branch tip. By determining a uniform distance for sampling, this allowed for observation of wood anatomical characteristics while accounting for any differences due to allometry. In addition, one sample was taken from the base of each shrub aiming at the largest and oldest branch of the individual to estimate shrub age.

B. SAMPLE PREPARATION

1. Dendrochronology

Transversal cuts of the samples taken from the base of each shrub were sanded in a graded series from 150 to 800 grit, polishing the surface to make the growth rings as visible as possible. These samples were further used to estimate shrub and branch age using dendrochronological methods.

Three radials paths of shrub rings were measured for each sample; Shrub Ring Widths (SRWs)[µm] for apical cuts were measured in ImageJ and SRWs of each basal shrub sample were measured using a TSAP measurement table.

SRWs were measured in a radial file from pith to bark to create a chronology series. Those chronology series were then cross dated using the statistics program COFECHA. There are several parameters within COFECHA that help indicate whether ring width samples are an acceptable cross-date match. Gleichläufigkeit (Glk) indicates the similarity between the growth regression of two ring width series, the T value (TV) indicates significance of correlation and the Cross Date Index (CDI) incorporates both the Glk and TV (Chan et al., 2013). Therefore, in addition to visual verification, samples that satisfied one of the following were considered successfully cross dated: Glk >70%, CDI >10, TV>3,0 (Rinntech, 2003). Once the three radial paths of each sample were successfully cross dated, the average was calculated for data analysis.

2. Wood anatomy

Transversal cuts of the *J. communis* and *C. oromediterraneus* samples taken 20 cm from the apical tip of each branch underwent histological preparation for microscopic observation of

woody tissue. As the angiosperm *C. oromediterraneus* has a more complex vascular structure, radial and tangential cuts were also taken to assist in the anatomical identification of the tracheary elements.

Making the thin cuts necessary for histological analysis can easily damage woody tissue. To avoid this, samples were embedded in paraffin blocks which provide them with the mechanical support necessary to obtain a clean thin cut.

2.1 Paraffin-embedding

Samples were placed in cassettes and dehydrated using a graded series of alcohol solutions and xylene substitute. This process removes any excess moisture as well as degrades non-lignin tissue, allowing for a clear observation of anatomical features. After dehydration, two cycles of paraffin immersion allow for full saturation of paraffin into the woody tissue. Once this process was completed, the samples were embedded into paraffin blocks using a Shandon HistoCentre 2 paraffin embedding station courtesy of the Medicina Legal, located on the campus of the University of Coimbra.

Samples in paraffin blocks were cut between 7-12 micron thick using a MICROM HM 340 E rotary microtome. The cuts were placed in a warm bath between 32-34ºC, facilitating the transfer to a microscope slide, after which they were left in a drying oven at 50ºC for at least 24 hours. Once dried, microscope slides were placed in a series of bioclear (two 100% solutions at 10 min. each) and ethanol (two 100% solutions at 2 min. each) solutions to remove any excess paraffin. After a quick rinse with distilled water to remove excess chemicals, samples were placed in a dye solution (40mg safranin, 150 mg astrablue, 100mL distilled water and 2mL acetic acid) for 10 minutes. Safranin dye stains lignified tissue while astrablue stains non-lignified tissue such as cellulose and starches, facilitating observation of the different tissue types (Zimowski et al., 2014).

2.2 Imaging

Images were taken from the histological preparations using the Leica DM4 M imaging microscope at magnifications x20 and x40. Three radial paths per sample were imaged in sections. In *C. oromediterraneus* samples radial paths were comprised of all cells within at least two ray parenchyma radial paths and between pith and cambial meristem. The plugin “stitching” as used in image analysis software ImageJ to compile the sections and compose images of the complete radial paths to be measured.

2.3 Wood anatomical measurements

To calculate the average lumen area (ALA), maximum lumen area (MLA) and hydraulic conductivity of *J. communis*, three radial paths of tracheids were measured per ring of each individual (fig. 11). To calculate the same parameters for *C. oromediterraneus* all tracheary elements within a selected section were measured for three sections per ring of each individual

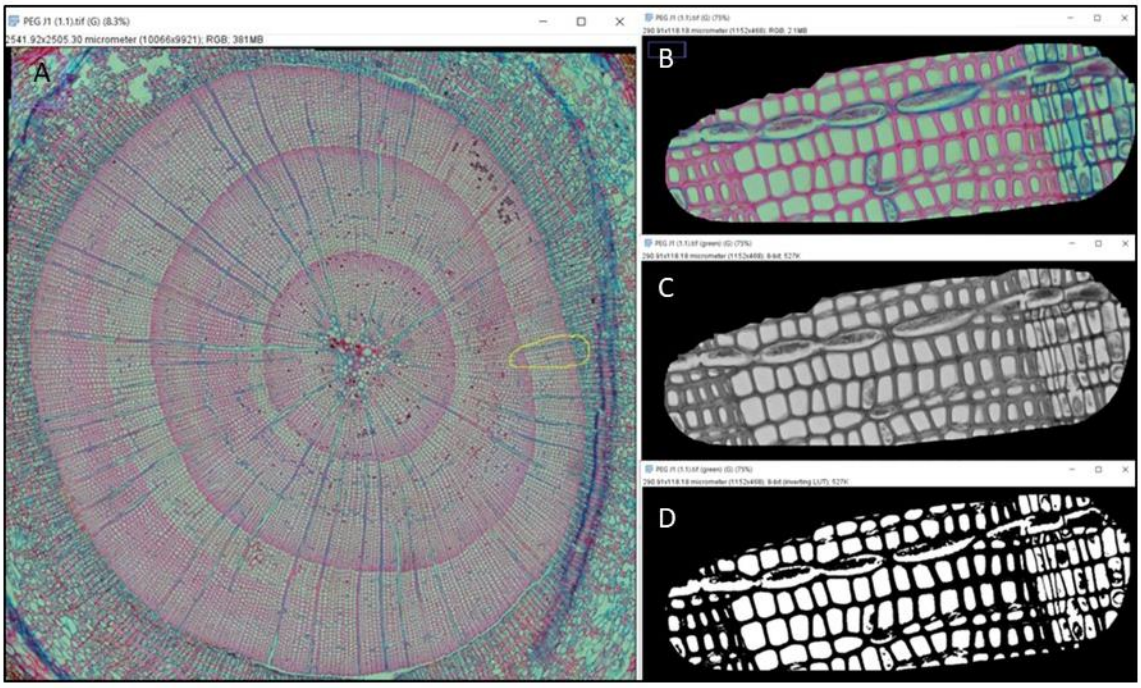

Figure 11. Selection of radial file of a growth ring within a Juniperus communis subsp. alpina cross-section for hydraulic conductivity measurements (A, B). Processing for image analysis by splitting color channels, selecting the green channel (C) and adjusting the brightness

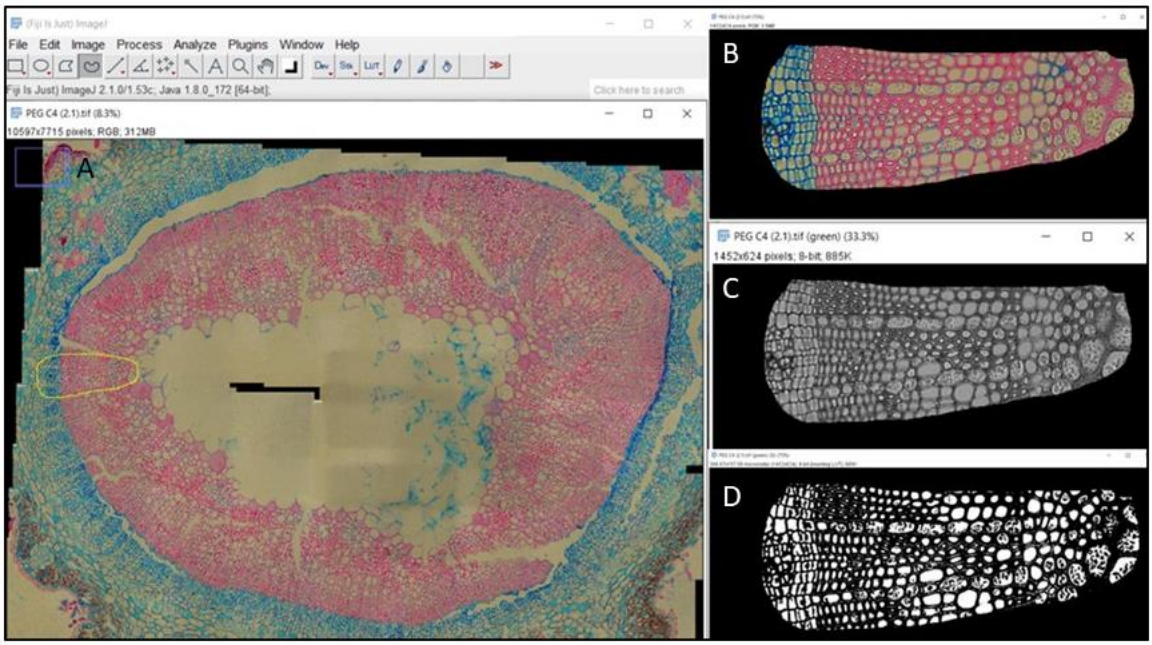

Figure 12. Selection of radial section of a growth ring within a Cytisus oromediterraneus cross-section for hydraulic conductivity measurements (A, B). Processing for image analysis by splitting color channels, selecting the green channel (C) and adjusting the brightness & contrast (D) to best display the contrast between cell lumen and cell wall.

(fig. 12). Vascular tracheids were sufficiently abundant in *C. oromediterraneus* individuals to potentially affect hydraulic conductivity estimation and therefore were also included in measurements (Schirarend, 2008). The process of obtaining conduit lumen area measurements using image analysis starts by splitting the color channels of the image and selecting the green channel which results in a black & white image that displays the best contrast between cell lumen and cell wall (figs. 11, 12). Then an automatic threshold is selected which designated pixels to either 0 (Black) or 255 (White) to distinguish between foreground and background, or in this case lumen and cell wall, respectively. The desired tracheary cells were then selected using the "analyze particles" plugin from ImageJ, which calculates the area of each vessel lumen [m^2] (figs. 13, 14).

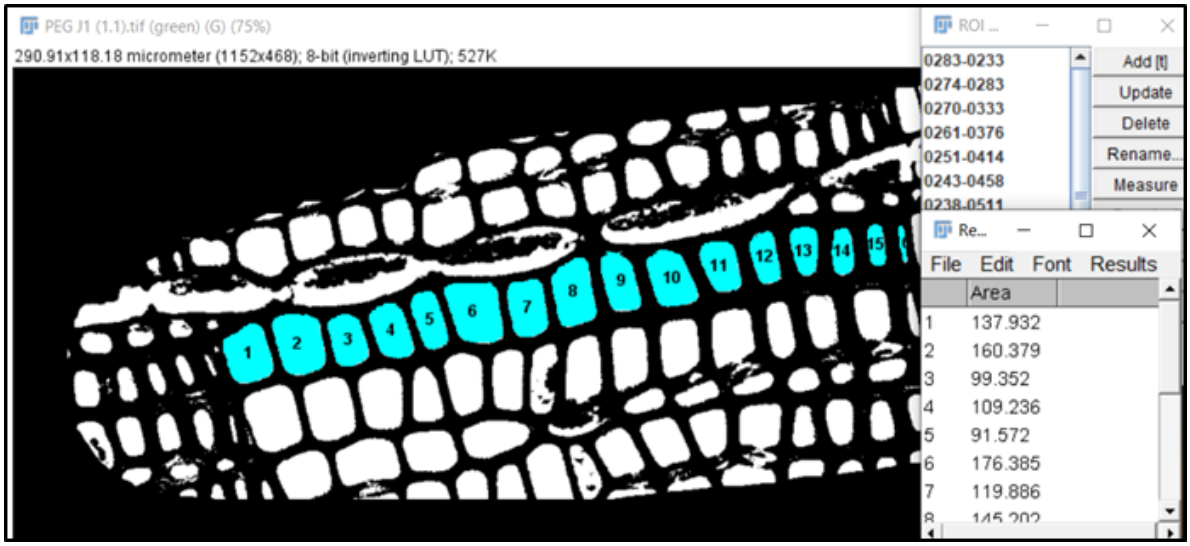

Figure 13. Labelling of tracheary elements in a growth ring of Juniperus communis subsp. alpina as Regions of Interest (ROI) and measurement of tracheary element areas for hydraulic conductivity calculations.

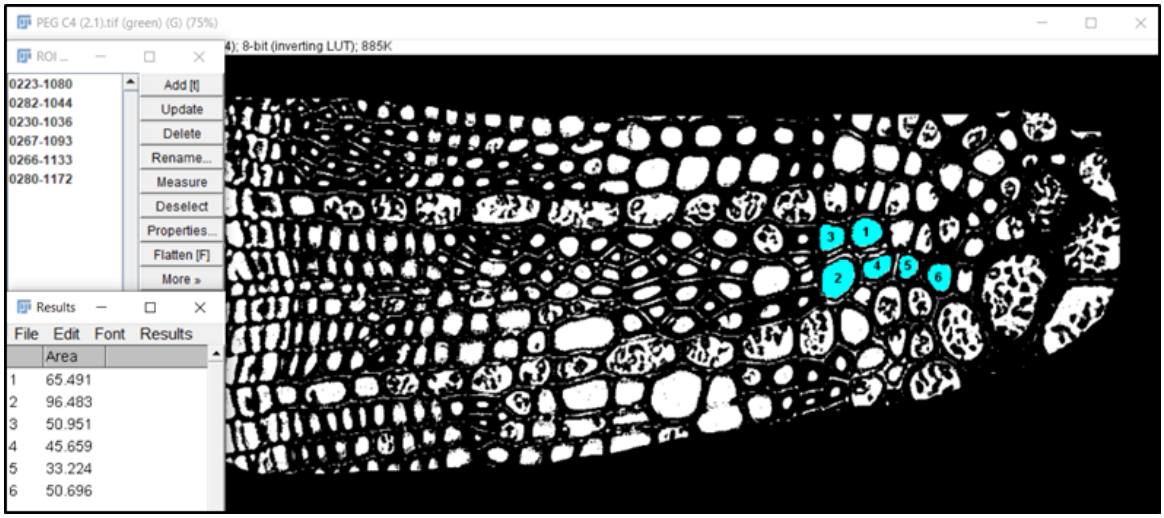

Figure 14. Labelling of tracheary elements in a growth ring of Cytisus oromediterraneus as Regions of Interest (ROIs) and measurement of tracheary element areas for hydraulic conductivity calculations.

Hydraulic conductivity is a function of inner conduit diameter to the fourth power and therefore, directly related to lumen diameter (Scholz et al., 2013; Sperry & Hacke, 2004). The diameter was calculated from the vessel area of each conduit vessel using equation 1:

$$D = \sqrt{\frac{4A}{\pi}} \qquad \text{Equation 1}$$

where D is the diameter and A, area.

To strengthen the role of conductive cells with larger conduits, which are either earlywood tracheids in *J. communis*, or vessels in *C. oromediterraneus*, the hydraulic diameter ($H_{D)}$ [µm] was calculated using equation 2:

$$D_H = \left(\frac{\sum D^4}{N}\right)^{\frac{1}{4}} \qquad \text{Equation 2}$$

where N is the number of conduits.

The hydraulic diameter was then used to calculate the hydraulic conductivity (K_H) [$m^4/MPa^{-1} \times s^{-1}$] (equation 3) and lumen resistivity (R_L) [MPa × s/m^{-4}] (equation 4) of each ring based on the Hagen-Poiseuille law:

$$K_H = \frac{\pi D^4}{128\,\eta} \qquad \text{Equation 3}$$

$$R_L = \frac{128\,\eta}{\pi D^4} \qquad \text{Equation 4}$$

where η is the viscosity index of water (1.002×10^{-9}MPa s at 20ºC).

R_L is calculated as the inverse of K_H and represents the individual's vulnerability to embolisms based on the size of the conduits and thus, is also related to conduit diameter (Pittermann & Sperry, 2003; Sperry et al., 2005). All equations were taken from Scholz et al. (2013).

Most individuals only had one replicate measurement for hydraulic conductivity parameters due to the labor-intensive nature of the image analysis process. However, some had more than one replicate measurement, and this was accounted for in statistical analysis.

C. DATA ANALYSIS

1. Climate data

In the climatic data obtained from IPMA, the monthly minimum and maximum temperatures were missing for several months in 2014 and 2015. Those values were substituted by using the average of the missing months from all other sample years. Data for precipitation, minimum and maximum temperatures was then loaded in the statistical environment Brodgar to calculate correlation matrices and Variance Inflation Factor (VIF) values for the climate variables. This information allows us to determine which explanatory variables are highly correlated and thus, might confound significance values. Explanatory variables only presented collinearity when data for all climate variables for all months was run together. Thus, in data analysis models did not simultaneously include all climate variables.

2. Pearson's Correlations

A Pearson's correlation test was run in R for the variables measured in the individuals from each species by site. Correlation coefficients may range between -1 and 1; the further the coefficient value from zero, the more correlated the variable. A positive coefficient indicates a positive relationship between the two variables while a negative coefficient indicates a negative relationship. Having a sample set with individuals that are positively correlated ensures the results will accurately reflect the growth of that species in the overall site. Those that are negatively correlated are either not exhibiting similar physiological responses to external conditions or have been improperly measured. Therefore, individuals that presented a moderate negative correlation with other individuals from the same species and site were removed from analysis.

3. Two-way ANOVAs and t-tests

Shrub parameters like size (height and volume), age (basal and apical), SRW (basal and apical), ALA, MLA, and K_H, were tested for normality using a shapiro test. A log transformation was the most appropriate for all variables except ALA to produce a normal data distribution. 2-way ANOVAs were performed with Tukey Honest Significant Differences (HSD) posthoc outputs to determine whether site, species and the interaction significantly accounted for variation in size, age (basal and apical), SRW (basal and apical), ALA, MLA, and K_H. Additionally, one sample t-test was used to test for significant differences in SRW growth in the last five years for both species.

4. Generalized Additive Models (GAMs)

Since the addition of explanatory environmental variables are expected to influence the prediction of the response variable in a relationship which may not necessarily be linear, Generalized Additive Models (GAMs) with a Gaussian distribution were the most appropriate to analyze the data (Olano et al., 2013).

Measurements for SRW and wood anatomy were log transformed to reflect a normal distribution and then merged with field and climate data in R using the 'base' package. Since the earliest climate data available was from 1968, SRWs dated earlier than this year were excluded from the GAM analysis. Initially, response variables were run in GAMs using the 'mgcv' package with individual monthly total precipitation, and average monthly minimum and maximum temperature. SRW and wood anatomy were then further analyzed by species and site using a GAM with the variables year and cambial age fit with spline curves and set as random factors. This is to ensure the results reflect response to climatic conditions and not differences that may be due to allometry or shrub age (Rodriguez-Zaccardo et al., 2019). In addition, as some individuals had more than one replicate measurement, the variable individual was also set as a random factor to remove the statistical weight that extra data may present.

The model was checked to meet the assumption for heteroskedasticity, which is defined as having data where the standard errors of a variable are non-constant. The data did not present heteroskedasticity, therefore the variation in the residual errors were constant and predictable, and the data was robust enough from which to draw conclusions. All explanatory climate variables were fit with a spline smoothing curve and plugged into the GAM using the principle of parsimony to find the best model fit, which was indicated by the lowest AIC value.

RESULTS

Shrub size and age

Plant species was a significant factor affecting shrub size ($p < 0.001$, table A1), and on average, *J. communis* shrubs were significantly larger than *C. oromediterraneus* (table 1). The interaction of plant species and site on shrub size was not significant ($p = 0.08$, table A1). Although not significant, when comparing sampling sites *J. communis* shrub size was smallest at the highest elevation site (COB, 6.05 m^3, table 1), and the largest individuals were located at the lowest elevation (NSA, 12.45 m^3, table 1). On the contrary, *C. oromediterraneus* shrubs size was largest in the highest site (COB, 3.27 m^3, table 1) and smallest in the lowest site (NSA, 1.94 m^3, table 1).

Table 1. Shrub volume, age, and ring-width (SRW – shrub ring width) of Juniperus communis subsp. alpina and Cytisus oromediterraneus. Data are mean ± SE.

Site	Elevation (m)	Sample size	Shrub volume (m^3)		Shrub age (years)		SRW (µm)	
			JUNIPERUS	CYTISUS	JUNIPERUS	CYTISUS	JUNIPERUS	CYTISUS
COB	1872	8	6.05 ± 1.11	3.27 ± 1.05	18 ± 3	23 ± 1	482 ± 85	449 ± 62
PEG	1790	8	6.97 ± 0.93	2.37 ± 0.54	72 ± 12	12 ± 2	255 ± 32	1026 ± 201
NSA	1563	8	12.45 ± 2.24	1.94 ± 0.20	22 ± 3	12 ± 1	430 ± 52	605 ± 49

The two-way ANOVA showed site ($p < 0.01$), species ($p < 0.001$) and the interaction between site and species ($p < 0.001$) to be significant factors on variation in shrub age (table A2). On average, the youngest *J. communis* individuals were found in the highest elevation site (COB, 18 years, table 1), and the oldest individuals were in the westernmost site (PEG, 72 years, table 1). The oldest *C. oromediterraneus* individuals were found in COB (23 years, table 1), while in PEG and NSA there were no significant differences in the average age ($p < 0.979$, 12 years, table 1).

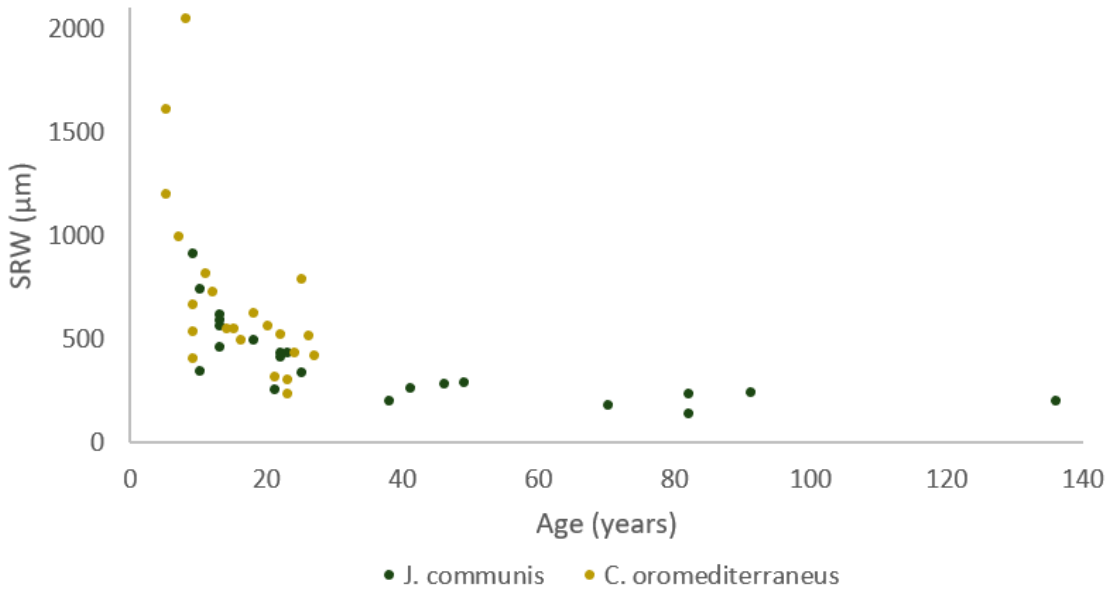

Figure 15. Relation between age and SRW for Juniperus communis subsp. alpina and Cytisus oromediterraneus from all three sampling sites.

SRW and average shrub age presented a significant negative relationship in both study species (correlation coefficient = -0.82, $p < 1.08e\text{-}12$, table A3), with smaller rings in older individuals and larger rings in younger individuals (fig.15).

Shrub ring width

A total of 894 basal rings were measured for *J. communis*, and 377 basal rings for *C. oromediterraneus*. Shrub species and interaction between site and species had a significant effect on shrub ring width (SRW, $p < 0.001$, table A4). *J. communis* in COB presented the largest SRW with an average value of 482 µm, while *J. communis* in PEG had the smallest average SRW (255 µm, table 1), although the 2-way ANOVA and Tukey posthoc test did not detect significant differences between sites for this species (table A4). In contrast, the average SRW of *C. oromediterraneus* individuals was smallest in COB (449 µm), and largest in PEG (1026 µm, table 1), and significantly different between them ($p < 0.01$, table A4). Significant differences were also found between both species in PEG ($p < 0.001$, table A4).

There was a positive temporal trend in SRW for both species (figure 16, table A5). One-way t-tests analysis by site and species indicated a significant increase in *J. communis* SRW from 2015-2019 in COB; in the lower two sites, NSA and PEG, there was a significant increase in SRW in four of the five most recent study years (table A5). *C. oromediterraneus* SRW did not present any significant increase in COB but did show a significant increase in PEG in all five most recent study years (figure 17, table A5). *C. oromediterraneus* SRW growth in NSA showed a significant increase from 2015-2018, and growth in the most recent year in the study, 2019, was marginally significantly ($p < 0.0663$, table A5).

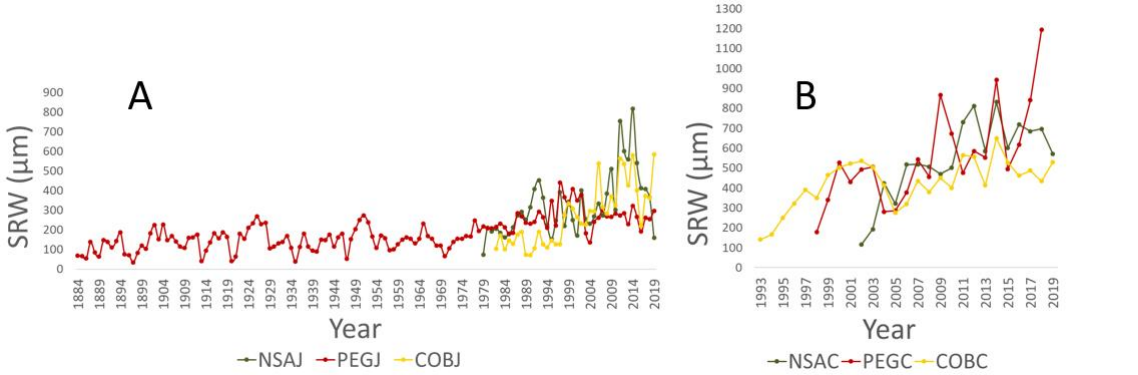

Figure 16. Average growth curves of Juniperus communis subsp. alpina (A) and Cytisus oromediterraneus (B) per site. SRW – Shrub Ring Width.

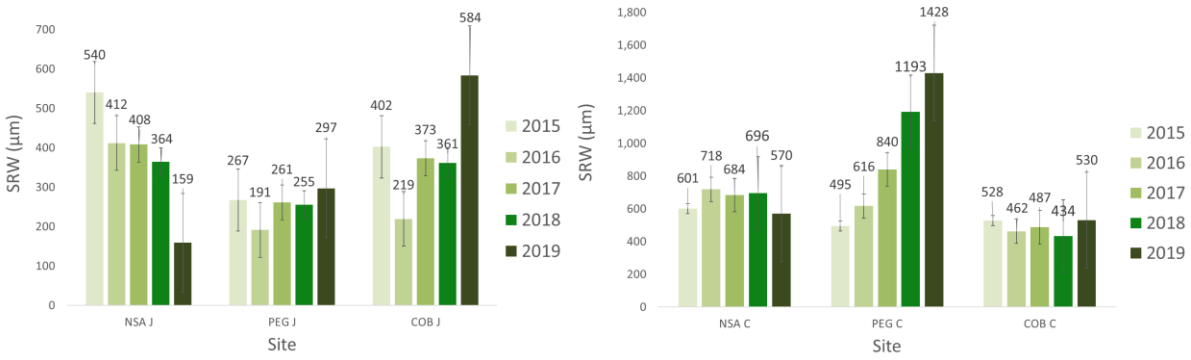

Figure 17. Average SRW of (A) Juniperus communis subsp. alpina and (B) Cytisus oromediterraneus per site from 2015-2019. SRW – Shrub Ring Width.

GAM analyses revealed interspecific and intraspecific differences in the factors most influencing SRW (table 2). For *J. communis*, SRW was most influenced by average maximum temperatures in May, September and October in COB; by precipitation in October, average minimum temperature in March and April, and average maximum temperature in February and December in PEG; and by July minimum temperatures in NSA (table 2). SRW in *C. oromediterraneus* was most influenced by April precipitation and December maximum temperatures in COB; by precipitation in April, October and November in PEG; and by precipitation in July, September and October in NSA (table 2).

Table 2. Results of the generalized additive models (GAM) analysis for shrub ring width (SRW) in Juniperus communis subsp. alpina and Cytisus oromediterraneus.

J. Communis

COB				
SRW	Estimate	SE	F	P
Intercept	5.6825	0.1377	41.27	2.00E-16
May Max T	1	1	15.598	0.0002
Sep Mat T	6.329	7.384	2.912	0.0086
Oct Max T	8.5	8.876	4.42	0.0001

PEG				
SRW	Estimate	SE	F	P
Intercept	5.3463	0.1478	36.18	2.00E-16
Oct P	4.032	4.913	2.481	0.0431
Mar Min T	1.575	1.948	3.629	0.0223
Apr Min T	3.477	4.285	3.769	0.0043
Feb Max T	2.087	2.591	7.096	0.0004
Dec Max T	4.156	5.034	4.431	0.0007

NSA				
SRW	Estimate	SE	F	P
Intercept	6.0499	0.1864	32.45	2.00E-16
Jul Min T	7.6577	7.963	2.247	0.02

C. Oromediterraneus

COB				
SRW	Estimate	SE	F	P
Intercept	5.9581	0.1304	45.68	2.00E-16
Apr P	1	1	7.834	0.0066
Dec Max T	1.424	1.572	4.865	0.0101

PEG				
SRW	Estimate	SE	F	P
Intercept	6.8397	0.2067	33.09	2.00E-16
Apr P	1	1	4.876	0.0314
Oct P	1	1	12.673	0.0008
Nov P	2.973	3.652	5.05	0.0021

NSA				
SRW	Estimate	SE	F	P
Intercept	6.2775	0.1742	36.03	2.00E-16
Jul P	2.775	3.259	3.737	0.0150
Sep P	3.164	3.799	5.586	0.0007
Oct P	1	1	10.585	0.0020

Wood anatomy analyses

A total of 145 apical rings were measured for *J. communis*, and 84 apical rings for *C. oromediterraneus*. Site, species and the interaction of both were all significant factors affecting branch age 20 cm from the apical tip ($p<0.001$, table A6). *J. communis*, on average, showed fewest rings in COB (4 years) and the most in PEG (7 years, table 3). Significant differences were found for this species between COB and PEG and between NSA and PEG (table A6). The branch age of *C. oromediterraneus* was highest in COB (5 years) and lowest in PEG (2 years, table 3). Significant differences were found between all sites for this species (table A6). Also, differences in branch age between both species were found in the three studied sites (table A6).

The 2-way ANOVA did not find site, species or the interaction between them to be significant factors for average lumen area (ALA, table A7). Values for ALA ranged between 71 and 84 μm^2 for all species and sites (table 3).

Table 3. Apical branch age (20 cm below the tip), average lumen area (ALA), maximum lumen area (MLA), branch ring width (BRW) and hydraulic conductivity (KH) of Juniperus communis subsp. alpina and Cytisus oromediterraneus. Data are mean ± SE.

Site	Elevation (m)	Sample size	Apical branch age		ALA (μm^2)		MLA (μm^2)		BRW (μm)		K_H ($m^4\ MPa^{-1}\ s^{-1}$)	
			JUNIPERUS	CYTISUS	JUNIPERUS	CYTISUS	JUNIPERUS	CYTISUS	JUNIPERUS	CYTISUS	JUNIPERUS	CYTISUS
COB	1872	8	4 ± 0.4	5 ± 0.8	83 ± 4	84 ± 7	194 ± 9	670 ± 73	401 ± 28	221 ± 30	$1.26 \times 10^{-8} \pm 3.06 \times 10^{-9}$	$1.16 \times 10^{-7} \pm 4.59 \times 10^{-8}$
PEG	1790	8	7 ± 1.5	2 ± 0.5	75 ± 4	80 ± 8	158 ± 8	544 ± 46	217 ± 19	218 ± 24	$2.04 \times 10^{-9} \pm 6.70 \times 10^{-10}$	$6.53 \times 10^{-8} \pm 4.67 \times 10^{-8}$
NSA	1563	8	5 ± 0.5	3 ± 0.9	71 ± 6	77 ± 6	156 ± 12	490 ± 42	278 ± 25	262 ± 29	$5.51 \times 10^{-9} \pm 2.18 \times 10^{-9}$	$6.30 \times 10^{-8} \pm 2.76 \times 10^{-8}$

The 2-way ANOVA showed that both site and species had a significant effect ($p<0.001$) on maximum lumen area (MLA), with the interaction being marginally significant ($p=0.06$, table A8). MLA of *J. communis* had the largest values in the highest elevation site COB (194 μm^2, table 3), with values in COB significantly higher than in the other two sites (table A8). The smallest MLA for *J. communis* individuals were found in NSA (156 μm^2, table 3). *C. oromediterraneus* had the largest MLA in COB (670 μm^2), and the smallest in NSA (490 μm^2, table 3), values significantly different according to the 2-way ANOVA and Tukey's posthoc test (table A8). Also, significant differences in MLA between both species were found in the three studied sites (table A8).

Hydraulic conductivity (K_H) was significantly affected by site and species ($p<0.001$, table A9) but an interaction between both factors was not detected. Significant differences were found between K_H in PEG and COB ($p<0.001$), and marginally significant between PEG and NSA ($p<0.054$, table A9). K_H for *J. communis* and *C. oromediterraneus* was highest in COB, with values of 1.26×10^{-8} and 1.16×10^{-7} $m^4\ MPa^{-1}\ s^{-1}$, respectively. For *J. communis* the lowest K_H was found in NSA, with 5.51×10^{-9} $m^4\ MPa^{-1}\ s^{-1}$ (table 3). K_H was significantly higher for *C. oromediterraneus* than for *J. communis* (table 3).

Branch ring width (BRW) was significantly affected by site ($p < 0.001$), species ($p < 0.05$) and the interaction between site and species ($p < 0.01$, table A10). Although significant differences were found between PEG and NSA ($p < 0.01$), and PEG and COB($p < 0.01$), there was no significant difference between the highest elevation site NSA and the lowest elevation site COB ($p < 0.989$). There was a significant difference in BRW between *J. communis in* COB and PEG ($p < 0.001$, table A10).

Based on the GAM analyses (table 4), K_H of *J. communis* appeared to be most influenced by February precipitation in COB, by September precipitation in PEG and by March average minimum temperatures in NSA. K_H of *C. oromediterraneus* was influenced by March precipitation and maximum temperature in COB; and by June maximum temperature in PEG and NSA.

Table 4. Results of the generalized additive models (GAM) analysis for hydraulic conductivity (K_H) in Juniperus communis subsp. alpina and Cytisus oromediterraneus.

J. Communis

COB				
K_H	Estimate	SE	F	P
Intercept	-19.1958	0.3505	-54.77	2.00E-16
Feb P	1	1	14.9	0.0008

PEG				
K_H	Estimate	SE	F	P
Intercept	-18.8791	0.8119	-23.25	2.00E-16
Sep P	1.81E+00	1.842	4.185	0.0263

NSA				
K_H	Estimate	SE	F	P
Intercept	-22.73	1.75	-12.99	1.88E-12
Mar Min T	1.976	1.999	12.748	0.000148

C. Oromediterraneus

COB				
K_H	Estimate	SE	F	P
Intercept	-18.368	0.2939	-62.49	2.00E-16
Mar P	1.502	1.752	18.59	0.0010
Mar Max T	1	1	10.82	0.0040

PEG				
K_H	Estimate	SE	F	P
Intercept	-21.36	1.07	-19.96	1.46E-11
Jun Max T	1.957	1.991	14.709	0.0003

NSA				
K_H	Estimate	SE	F	P
Intercept	-22.38	2.55	-8.779	1.85E-05
Jun Max T	1	1	5.542	0.0451

The relation between branch ring width (BRW), ALA and MLA in *J. communis* and *C. oromediterraneus*, considering all sampling sites together, is shown in figure 18. In general, the relation between the three parameters is positive, that is, larger BRW are associated with larger ALA and MLA. However, the strongest link is between ALA and MLA, with a linear relationship and a R^2 of 0.90 and 0.76 for *J. communis* and *C. oromediterraneus*, respectively (fig. 18). There is no clear relation between ALA, MLA and K_H in neither of the two species (fig. 19). The relation between BRW and KH for both species fits an exponential curve with an R^2= 0.79 for *J. communis* (notice the three outliers marked in the graph), and an R^2 = 0.77 for *C. oromediterraneus* (fig. 19).

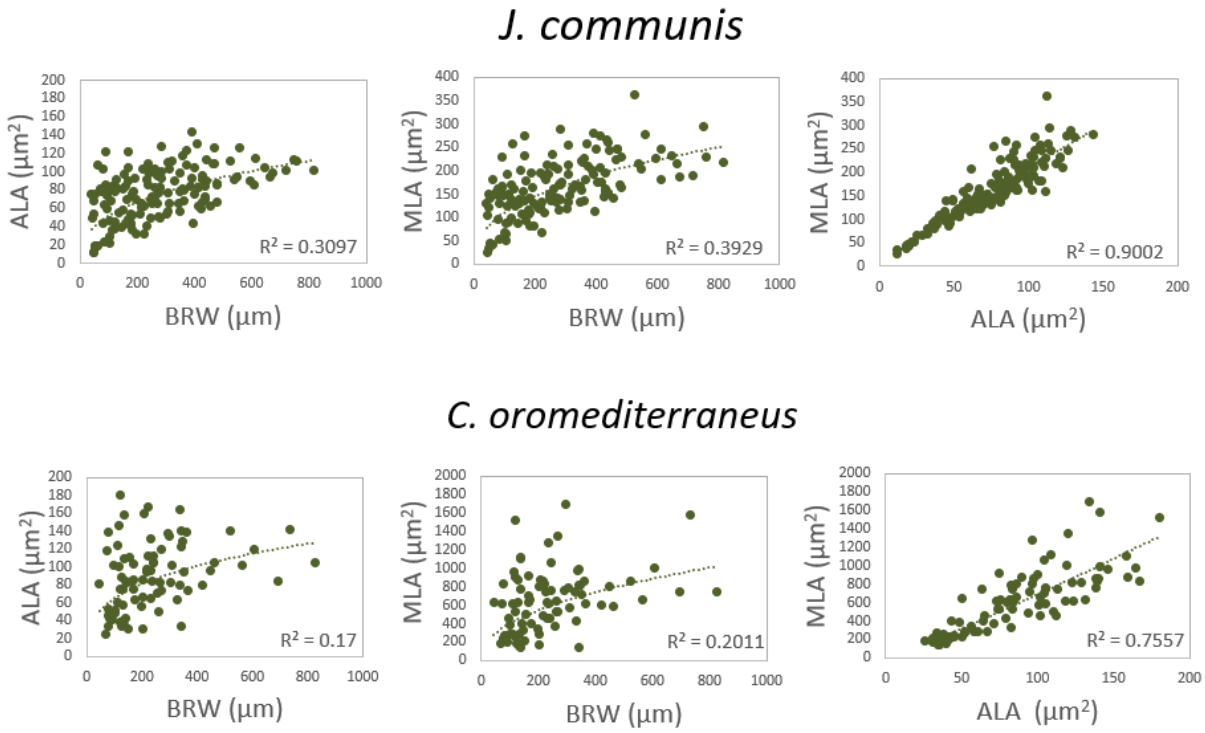

Figure 18. Relation between branch ring width (BRW), average lumen area (ALA) and maximum lumen area (MLA) and Juniperus communis subsp. alpina (top) and Cytisus oromediterraneus (bottom).

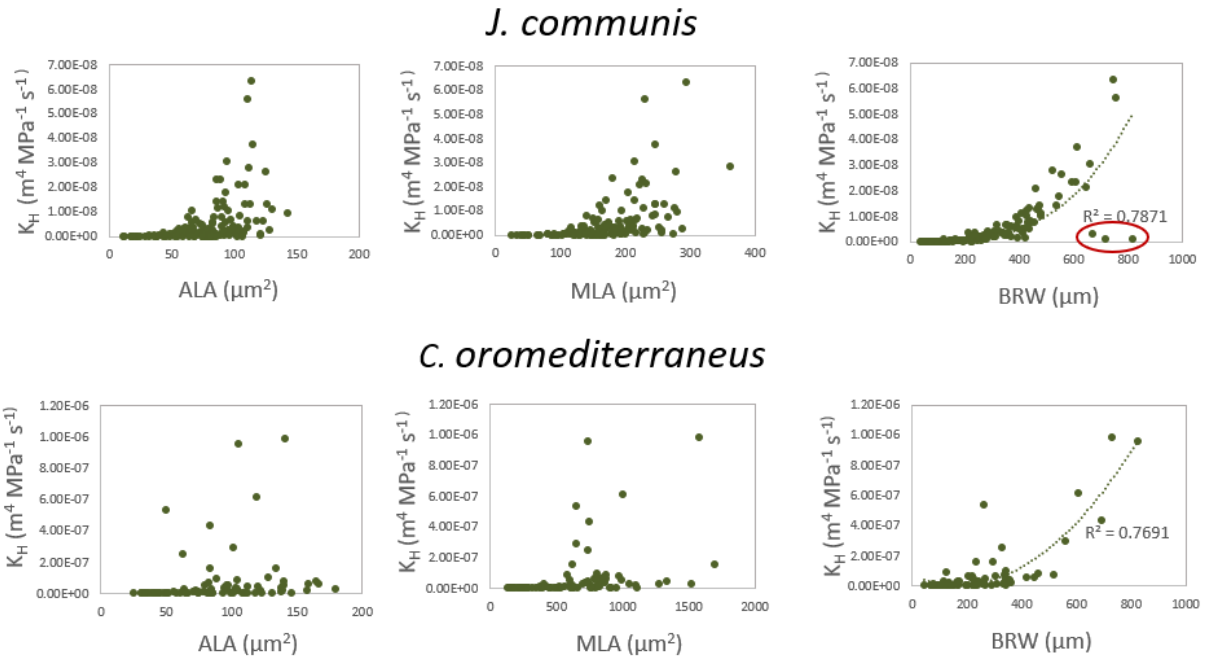

Figure 19. Relation between average lumen area (ALA), maximum lumen area (MLA) and branch ring width (BRW) with hydraulic conductivity (K_H) in Juniperus communis subsp. alpina (top) and Cytisus oromediterraneus (bottom). Data outliers are circled in red.

DISCUSSION

Shrub size, age and growth

The growth habit of both species is very different (fig. 20) and probably accounted for the differences observed in size, since *J. communis* individuals were much larger than *C. oromediterraneus* individuals, as statistically confirmed via 2-way ANOVA. This is likely explained by the propensity for phenotypic plasticity and procumbent nature of *J. communis* (Myers-Smith et al., 2015), which may allow a larger horizontal growth due to strong winds and other vertical growth constraints. Both species also presented different patterns in shrub size along the three study sites. For *C. oromediterraneus* the largest individuals were found in the highest elevation site (COB), which might be explained by a combination of release from competition and eastern orientation. Shrublands in NSA were quite dense with little space between individuals, but as elevation increases vegetation becomes sparser, resulting in more isolated shrubs with grassland or bare soil between them. Additionally, COB results a better site than PEG likely due to its southeastern orientation, which better fits the bioclimatic preferences of *C. oromediterraneus* for warmer climates (Jansen, 2011). On the other hand, *J. communis* shrub size showed an opposite trend, decreasing with increasing altitude, reflecting that both shrub species' growth might respond differently to climatic factors, competition and, likely, herbivory (Thomas et al., 2007). Growth constraint by low minimum temperatures and strong winds characteristic of the alpine region of Estrela may have affected *J. communis* growth in COB and PEG. The largest *J. communis* individuals were found in the lowest site (NSA), indicating a better growth probably due to warmer conditions and, when surrounded by a denser shrubland, more protection against browsing by large herbivores (Markó et al., 2011; Thomas et al., 2007).

Figure 20. Growth habit of Juniperus communis subsp. alpina (foreground) compared to Cytisus oromediterraneus (background) in the alpine region of Estrela.

Concerning the age structure of the studied populations, results indicate that there are differences between *J. communis* and *C. oromediterraneus*, as well as between sites. The

oldest *J. communis* individuals were found in the westernmost site (PEG), supporting that this site presented more favorable conditions for *J. communis* establishment, either due to a more temperate climate, or to little fire disturbance in this area. In this sense, the presence of young *C. oromediterraneus* individuals in PEG is very interesting as it could indicate a western expansion of this species. Indeed, vegetation maps from 2005 do not report *C. oromediterraneus* in this area (ICNF communication; figure A1). However, a more thorough study is needed to make any definitive conclusions on *C. oromediterraneus* shifts in distribution in this region.

Interestingly, there is a clear increase in shrub width ring in the last five years, showing the positive response of both species to current warming; this response has been found to be more common in colder climates than in the Mediterranean since summer drought imposes and important limitation to plant growth (Garcia-Cervigón et al., 2012).

Overall, SRW was smaller in *J. communis* than *C. oromediterraneus,* although this was site-specific. The interspecific differences in SRW might be due to differences in the age of the populations (older individuals for *J. communis* compared to *C. oromediterraneus*) and/or to a higher complexity and tissue specialization of angiosperm xylem anatomy that inherently results in more biomass. The difference in SRW between both species was particularly large in PEG where the difference in shrub age was also the largest between both species (72 ± 12 for *J. communis* and 12 ± 2 for *C. oromediterraneus*). *J. communis* showed an opposing trend between shrub age and average SRW, with smaller rings occurring in older individuals and larger rings in younger individuals. This is likely due to the variation in cambial activity and xylem formation with age (Vaganov et al., 2006; Li et al., 2013; Rodriguez-Zaccaro et al., 2019). However, the age effect is not the only explanation for the variation in SRW. Olano et al. (2013) suggests that secondary growth is highest at intermediate elevations. This is highlighted when comparing *C. oromediterraneus* from PEG and NSA, with similar age (12 years) but SRW much larger in PEG (1,020 µm) than in NSA (605 µm). This indicates that SRW is influenced by local conditions, which in Estrela can change in both a gradient with elevation as well as east-west orientation.

Shrub ring width and climatic signals

The temporal growth curves reflect the shrub growth response to the specific conditions of each year in each site. In general, dwarf shrubs often present high individual growth variability (Bär et al., 2006) however, when comparing the three sites and the common temporal period, there was a higher similarity of growth curves for *J. communis* than for *C. oromediterraneus*. This suggests that *J. communis* growth may be more responsive to macroclimatic conditions

common to the three sites and thus, will exhibit similar growth responses. The dissimilar response observed in *C. oromediterraneus* might be due to the young age of the shrubs, thus with less statistical power to crossdate, and a higher noise of individual growth. However, it can also indicate that *C. oromediterraneus* is more sensitive to microclimatic conditions, which are probably different among the three sampling sites. Despite the variability in growth curves among sites, there was a clear significant increase in shrub growth in the five most recent years which follows the current warming trend, thus, supporting our first hypothesis.

Overall, temperature had a more significant effect on SRW for *J. communis* while precipitation was more important for *C. oromediterraneus* growth, probably reflecting the different sensitivity to water availability in conifers and angiosperms, with conifers showing lower hydraulic conductivity, but higher resistance to cavitation (Brodribb et al., 2012). SRW was explained by slightly different climatic factors in the three studied sites, probably reflecting microclimatic differences. However, we must consider that SRW of all sampling sites was compared with climatic parameters measured in one single site, the meteorological station of Penhas Douradas, limiting our conclusions. Nonetheless, SRW of *J. communis* was sensitive to spring and autumn/winter temperatures, while *C. oromediterraneus* was sensitive to spring/summer and autumn precipitation. Spring and summer conditions, either of temperature or precipitation, are extremely important for the main growing season, while autumn temperature or precipitation can be important for a second growth peak before the winter dormancy.

The significance of spring and fall temperatures in SRW for *J. communis* has been previously shown in other Mediterranean mountains (Garcia-Cervigón et al., 2012). This result emphasizes the importance of air temperatures on the cambial activity (Garcia-Forner et al., 2019). An earlier increase in spring temperatures, and a late decrease of fall and winter temperatures can result in a longer growth season, which would inherently influence the temporal capacity for cambial development. For example, the functional significance of December maximum temperatures in PEG on *J. communis* SRW could indicate a reduction of the freeze-thaw events on embolism formation (Charrier et al., 2014; Pitterman & Sperry, 2003), and the possibility to maintain growth. From the growth curves it seems that in the last 5-10 years there has been an increase in the SRW of both species. This could be a consequence of the increasing temperatures observed in Estrela, increasing the length of the growing season, and thus with more time to produce cells to build the growth ring. However, a longer temporal record is necessary to confirm this apparent growth trend.

Other studies have found a strong signal of precipitation on *J. communis* growth in high elevation Mediterranean sites (Garcia-Cervigón et al., 2012), which was not verified in this

study. This may be explained by the position of Serra da Estrela in the transition zone between temperate and Mediterranean climates which results in more humid conditions, thus water being less limiting for *J. communis* growth. Interestingly, October precipitation was a significant factor in PEG, and may reflect the ability of fall precipitation to assist in the recovery from summer water stress (Garcia-Forner et al., 2019).

Water availability is essential for the resumption of cambial activity and ring formation (Garcia-Forner et al., 2019). Accordingly, spring and fall precipitation were the most important factors influencing *C. oromediterraneus*, indicating that water availability, and not temperature, was the main factor limiting growth in this species in the upper plateau of Serra da Estrela. The ability to produce large vessels in angiosperms is largely dependent on water availability, and the wider the vessels, the higher the capacity to transport water, allowing a higher photosynthetic activity and growth. It is interesting to note that, *C. oromediterraneus* SRW at the highest elevation (COB) was also influenced by December maximum temperatures, which may reflect the importance of winter temperature in the release from freeze-thaw stress.

Wood anatomical characteristics

The significant differences between sites and species in branch age 20 cm from the apical tip are interesting, as the selection of a predetermined distance from the apical tip was intended to control for this variability. This could, however, be due to alpine shrub species' propensity to develop growth anomalies such as discontinuous or missing rings in response to harsh conditions (Wilmking et al., 2011; Bär et al., 2006). More detailed studies on annual ring formation and growth for these species and sited should be conducted in order to elucidate this observed difference in ring numbers.

The relationship between BRW, ALA and MLA, for both *J. communis* and *C. oromediterraneus,* is best described by a saturation curve, meaning that the rate of increase in BRW is associated with a lower rate of increase of ALA and MLA. A growth ring needs to balance the lumen area, which is related to the capacity for water conduction, with mechanical structures that provide support, like cell wall thickness of tracheids, fibers, and reserve tissues, like parenchyma. Thus, wider rings probably invest relatively more space for mechanical strength, better stabilizing the lumen area. It is interesting to note that at lower ring widths ALA and MLA showed higher variability in *C. oromediterraneus* than in *J. communis,* which is likely due to the higher anatomical heterogeneity of hardwood compared to softwood.

The relationship between ALA and MLA for both species is better described by a linear curve. This indicates that MLA is largely influencing ALA. According to Scholz et al. (2013) few large

vessels may transport more water than several small vessels therefore, the MLA of a growth ring is likely to have a larger influence on the capacity for a plant individual's K_H than the ALA (Olano et al., 2013). MLA and K_H were higher in COB for both species; the higher MLA values at the highest altitude (COB) contradict the idea that colder climates generally induce more narrow vessels because they are more resistant to the freeze-thaw embolism (Olson et al., 2018). However, water availability also influences the MLA, and COB can have local characteristics like a soil with a higher water retention capacity, or more fog, which increases humidity and water availability.

The relation between ALA and MLA with K_H in both species showed no clear trend in both species, being more scattered in *C. oromediterraneus*. On the other hand, the relation between BRW and K_H for both species is well described by an exponential curve, meaning that at a certain threshold of ring-width there is a large increase in K_H. Notice that the calculation of K_H is considering all the lumen area of the growth ring, either from large or small tracheids, or vessels. Thus, ALA and MLA represents a fraction of the lumen area, while the BRW integrates better the lumen area along the growth ring. The exponential relation also indicates that wider rings can accommodate wider tracheids (or vessels) that have a large impact on the hydraulic conductivity. Additionally, and especially in the angiosperm vascular tissue, composed of several specialized tissue types, larger growth rings also provide the opportunity to develop larger fractions of non-conducting tissues, such as parenchyma, that may aid in the prevention of conduit embolisms, allowing for the development of larger vessels (Olano et al., 2013). Since few large conduits may conduct more water than several small ones at a function of the fourth power, the development of larger tracheary elements will inherently result in exponentially increasing levels of conductivity.

It is interesting to note that while *J. communis* and *C. oromediterraneus* displayed opposing elevational trends in shrub size, they both displayed higher K_H at higher elevations. This suggests that while the phenotypic plasticity of *J. communis* and *C. oromediterraneus* in response to harsh conditions may be species specific (Myers-Smith et al., 2015), the response of physiological processes such as K_H to climatic conditions may be similar across species.

Hydraulic conductivity and climatic signals

There were fewer climatic variables affecting hydraulic conductivity than those affecting SRW. Additional replicates of hydraulic conductivity would have probably allowed for more punctilious GAM results. Nonetheless, it is interesting to highlight that in *J. communis*, K_H was more sensitive to precipitation of early spring (COB) and early autumn (PEG), while SRW was more sensitive to spring and autumn temperature. Thus, the two parameters (K_H and SRW)

are integrating different climatic signals. Somehow it is expected that K_H would be more sensitive to water availability, if wider tracheids and vessels are expected to be produced when more water is available. The same rational applies for the effect of March precipitation and temperature on *C. oromediterraneus* K_H in COB, reflecting the importance of spring climatic conditions for resumption of growth and development of vessels (Garcia-Forner et al., 2019; Begum et al., 2013). Interestingly, while SRW of *C. oromediterraneus* is more sensitive to spring and autumn precipitation, K_H is more sensitive to spring and summer temperature. However, it is difficult to explain the positive relation of K_H and maximum temperature of June in PEG and NSA for *C. oromediterraneus*. Higher temperatures in the summer months increase evapotranspiration, and if there is a decrease in water availability, there is an increasing risk of embolism. However, supplementary water availability data such as evapotranspiration or soil humidity measurements would be needed to make further inferences on this.

The climatic data for this study was obtained from the highest station available in the area, Penhas Douradas, located at 1380 masl. However, all sampling sites used the same climatic data and were located above this elevation. Therefore, due to the effect of altitude in temperature and the marked effect of orientation in precipitation in Serra da Estrela, more detailed climatic data is suggested to produce more informative results. The placement of weather stations in different sites in Serra da Estrela would aid to understand better how microclimatic conditions change and the effect of these changes in the ecosystem. In addition, including evapotranspiration data, as well as a drought index, may provide a better indication of the effects of drought on hydraulic conductance and growth.

Something else to consider is the variation of xylem structure throughout an individual, both from apical tip to root and from younger to older vascular tissue. Rodriguez-Zaccardo et al. (2019) suggests using older branches for a more robust representation of overall hydraulic conductivity. In addition, experiments on conductance using pressure flow or other hydraulic conductivity proxies may give a more holistic and dynamic understanding of this process in Mediterranean alpine shrubs (Garcia-Forner et al., 2016). Other recommended supplementary analyses include tissue fraction and vessel density measurements, which may elucidate on the underlying mechanisms that influence cambial tissue formation in hardwood species.

CONCLUSION

The alpine shrub species in this study show a clear response to increasing temperature, with a positive growth trend over the last five years, corroborating the first hypothesis of this study. The GAM results indicate that spring and autumn temperature are the most important climatic

variables affecting the growth of *J. communis*, thus, partially confirming our second hypothesis. The increase in *C. oromediterraneus* growth seemed to be regulated by spring and autumn precipitation, which might be key to trigger cambial activity in this species. Additionally, *C. oromediterraneus* growth was more affected by spring and autumn precipitation than *J. communis*, thus confirming the higher drought resistance of the gymnosperm as stated in the third hypothesis. Decreasing precipitation might counteract the positive response to warming and impair shrub growth, but *J. communis* will be less affected by decreases in precipitation than *C. oromediterraneus.*

Although climate change is a prominent driver in the shift of plant species distribution, other factors such as changes in land use and grazing may also have a significant impact on seedling establishment and shrub cover (Garcia-Cervigón et al., 2012; Zimowski et al., 2014). Higher temperatures and drier conditions forecasted for the Mediterranean may lead to increases in the frequency of fire disturbance events in a region that is already impacted by fire during the dry summer months. Although species such as *C. oromediterraneus* favor an intense fire disturbance regime (Fernandez-Santos et al., 2004) other species such as *J. communis* may not exhibit the same preference or capability of recovery and succession (Thomas et al., 2007) which could lead to potential shifts in the mosaic of the alpine shrub ecosystems in Estrela. Since land management influences shrub cover, alterations in land management practices such as pastoralism can also lead to changes in species' distribution and composition (Desoto et al., 2010; Lu et al., 2019). Indeed, Estrela habitats dominated by *J. communis* and *C. oromediterraneus* spp. are dependent upon pastoralism practices and according to the European Red list of habitats, these practices are recommended for conservation of alpine and sub-alpine *J. communis* habitats (Jansen, 2011; ICN, 2006). In addition, Estrela pastoralism practices, which are also dependent on local vegetation composition, provide many economically important goods for the local population such as cheese and clothing (Jansen, 2011) and therefore, it is of economic interest to study how the structure of the alpine landscape in Estrela might change in response to increasing temperatures.

To the best of our knowledge, this study contributes with novel information on the response to climate change of alpine shrubs in the Mediterranean, which are much less studied than in colder regions. This is also the first study of its kind in Serra da Estrela, specifically, using dendrochronology and quantitative wood anatomy to study the secondary growth and infer the physiology of woody plants above the tree line in response to global warming. High elevation mountain plants are likely to be highly responsive to climate change (Bär et al., 2006), and alpine shrubs in Estrela have been proven to be applicable in dendroecological studies. Elevational increases of isotherms due to increasing temperatures will eventually result in a

reduction of alpine and boreal regions and inherently, a loss of the associated high elevation habitats. As these increases in temperature in concert with increasing drought conditions are likely to have a pronounced impact on Mediterranean mountainous regions, this study was of importance to better understand alpine plant response to global warming in the Mediterranean, useful to predict and mitigate the impact of climate change on plant species and communities in vulnerable regions such as these.

REFERENCES

Abrantes, J., Campelo, F., García-Gonzelez, I. & Nabais, C. (2012). Environmental control of vessel traits in Quercus ilex under Mediterranean climate : relating xylem anatomy to function. *Trees,* 27: 655–662. https://doi.org/10.1007/s00468-012-0820-6

Anadon-Rosell, A., Rixen, C., Cherubini, P., Wipf, S., Hagedorn, F., & Dawes, M. A. (2014). Growth and phenology of three dwarf shrub species in a six-year soil warming experiment at the alpine treeline. *PLoS ONE*, *9*(6). https://doi.org/10.1371/journal.pone.0100577

Anderegg, W. R. L., Schwalm, C., Biondi, F., Camarero, J. J., Koch, G., Litvak, M., Ogle, K., Shaw, J. D., Shevliakova, E., Williams, A. P., Wolf, A., Ziaco, E., & Pacala, S. (2015). Pervasive drought legacies in forest ecosystems and their implications for carbon cycle models. *Science*, *349*(6247): 528–532. https://doi.org/10.1126/science.aab1833

Bär, A., Bräuning, A., & Löffler, J. (2006). Dendroecology of dwarf shrubs in the high mountains of Norway - A methodological approach. *Dendrochronologia*, *24*(1): 17–27. https://doi.org/10.1016/j.dendro.2006.05.001

Bär, A., Pape, R., Bräuning, A., & Löffler, J. (2008). Growth-ring variations of dwarf shrubs reflect regional climate signals in alpine environments rather than topoclimatic differences. *Journal of Biogeography*, *35*(4): 625–636. https://doi.org/10.1111/j.1365-2699.2007.01804.x

Bergmeier, E., Zimowski, M., Leuschner, H. H., & Holger, G. (2014). *Age and diversity of Mediterranean dwarf shrublands : a dendrochronological approach along an altitudinal gradient on Crete*. *25*: 122–134. https://doi.org/10.1111/jvs.12067

Brodribb, T. J., Pitterman, J., & Coomes, D. A. (2012) Elegance versus speed: examining the compoetition between conifer and angiosperm trees. *International Journal of Plant Science,* 173(6): 673–694. DOI: 10.1086/666005

Butterfield, B. G., & Meylan, B. A. (1980). Three-dimensional structure of wood. In *Three-dimensional structure of wood*. https://doi.org/10.1007/978-94-011-8146-4

Camarero, J. J., Olano, J. M., & Parras, A. (2010). Plastic bimodal xylogenesis in conifers from continental Mediterranean climates. *New Phytologist*, *185*(2): 471–480. https://doi.org/10.1111/j.1469-8137.2009.03073.x

Carlquist, S. (1985). Vasicentric Tracheids As a Drought Survival. *Aliso*, *11*(1): 37–68. http://kbd.kew.org/kbd/detailedresult.do?id=71562

Carnicer, J., Coll, M., Ninyerola, M., Pons, X., Sánchez, G., & Peñuelas, J. (2011). Widespread crown condition decline, food web disruption, and amplified tree mortality with increased climate change-type drought. *Proceedings of the National Academy of Sciences of the United States of America*, *108*(4): 1474–1478. https://doi.org/10.1073/pnas.1010070108

Chan, M. H., Hu, S. T., Lin, H. C., & Fujimoto, N. (2013). Comparison of COFECHA and TSAPWIN from dendroclimatology for climate change and taiwan fir (*Abies kawakamii*) growth pattern in alpine central Taiwan. *Journal of the Faculty of Agriculture, Kyushu University*, *58*(1): 115–123.

Chapin, F. S., Sturm, M., Serreze, M. C., McFadden, J. P., Key, J. R., Lloyd, A. H., McGuire, A. D., Rupp, T. S., Lynch, A. H.,…& Welker, J. M. (2005). Role of land-surface changes in arctic summer warming. *Science*, *310*(5748): 657–660. https://doi.org/10.1126/science.1117368

Christensen, J.H., B. Hewitson, A. Busuioc, A. Chen, X. Gao, I. Held, R. Jones, R.K. Kolli, W.-T. Kwon, & P. Whetton, 2007: Regional Climate Projections. In: Climate Change 2007: The Physical Science Basis. Contribution of Working Group I to the Fourth Assessment Report of the Intergovernmental Panel on Climate Change. Cambridge University Press, Cambridge, United Kingdom and New York, NY, USA.

Copenheaver, C.A., Gärtner, H., Schäfer, I., Vaccari, F.P., & Cherubini, P. (2010). Drought-triggered false ring formation in a Mediterranean shrub. *Botany*, 88: 545–555. https://doi.org/10.1139/B10-029

Costa, J. C.; Aguiar, C.; Capelo, J.; Lousã, M.; Neto, C. (1998). Biogeografia de Portugal Continental. *Quercetea*. ISSN 0874-5250, p. 5-56. http://hdl.handle.net/10198/714

Desoto, L., Olano, J. M., Rozas, V., & De La Cruz, M. (2010). Release of Juniperus thurifera woodlands from herbivore-mediated arrested succession in Spain. *Applied Vegetation Science*, *13*(1): 15–25. https://doi.org/10.1111/j.1654-109X.2009.01045.x

Díaz-Varela, R. A., Colombo, R., Meroni, M., Calvo-Iglesias, M. S., Buffoni, A., & Tagliaferri, A. (2010). Spatio-temporal analysis of alpine ecotones: A spatial explicit model targeting altitudinal vegetation shifts. *Ecological Modelling*, *221*(4): 621–633. https://doi.org/10.1016/j.ecolmodel.2009.11.010

Elsen, P. R., Monahan, W. B., & Merenlender, A. M. (2018). Global patterns of protection of elevational gradients in mountain ranges. *Proceedings of the National Academy of Sciences of the United States of America*, *115*(23): 6004–6009.

https://doi.org/10.1073/pnas.1720141115

Fernández-Santos, B., Martínez, C., García, J. A., & Puerto, A. (2004). Postfire regeneration in Cytisus oromediterraneus: Sources of variation and morphology of the below-ground parts. *Acta Oecologica*, *26*(2): 149–156. https://doi.org/10.1016/j.actao.2004.03.011

Frahm, J.-P., & Gradstein, S. R. (1991). An Altitudinal Zonation of Tropical Rain Forests Using Byrophytes. *Journal of Biogeography*, *18*(6): 669-678 . https://doi.org/10.2307/2845548

Garcia-Cervigón, A. I., Olano, J. M., Eugenio Gozalbo, M., & Camarero J. J. (2012). Arboreal and prostrate conifers coexisting in Mediterranean high mountains differ in their climatic responses. *Dendrochronologia*, *30*(4): 279–286. https://doi.org/10.1016/j.dendro.2012.02.004

Garcia-Forner, N., Vieira, J., Nabais, C., Carvalho, A., Martínez-Vilalta, J., & Campelo, F. (2019). Climatic and physiological regulation of the bimodal xylem formation pattern in *Pinus pinaster* saplings. *Tree Physiology*, *39*(12): 2008–2018. https://doi.org/10.1093/treephys/tpz099

García, D., Zamora, R., Hódar, J. A., & Gómez, J. M. (1999). Age structure of *Juniperus communis* L. in the Iberian peninsula: Conservation of remnant populations in Mediterranean mountains. *Biological Conservation*, *87*(2): 215–220. https://doi.org/10.1016/S0006-3207(98)00059-7

Gazol, A., Camarero, J. J., Vicente-Serrano, S. M., Sánchez-Salguero, R., Gutiérrez, E., de Luis, M., Sangüesa-Barreda, G., Novak, K., Rozas, V., …& Galván, J. D. (2018). Forest resilience to drought varies across biomes. *Global Change Biology*, *24*(5): 2143–2158. https://doi.org/10.1111/gcb.14082

Jansen, J. (2011). *Managing Natura2000 in a changing world: The example of the Serra da Estrela (Portugal)* (Doctoral dissertation, Radboud University, Nijmegen, the Netherlands).

Kannenberg, S. A., Maxwell, J. T., Pederson, N., D'Orangeville, L., Ficklin, D. L., & Phillips, R. P. (2019). Drought legacies are dependent on water table depth, wood anatomy and drought timing across the eastern US. *Ecology Letters*, *22*(1): 119–127. https://doi.org/10.1111/ele.13173

Kudo, G., & Suzuki, S. (2003). Warming effects on growth, production, and vegetation structure of alpine shrubs: A five-year experiment in northern Japan. *Oecologia*, *135*(2): 280–287. https://doi.org/10.1007/s00442-003-1179-6

Li, X., Liang, E., Gričar, J., Prislan, P., Rossi, S., & Čufar, K. (2013). Age dependence of xylogenesis and its climatic sensitivity in Smith fir on the south-eastern Tibetan Plateau. *Tree Physiology*, *33*(1): 48–56. https://doi.org/10.1093/treephys/tps113

Lovisolo, C., & Schubert, A. (1998). Effects of water stress on vessel size and xylem hydraulic conductivity in Vitis vinifera L. *Journal of Experimental Botany*, *49*(321): 693–700. https://doi.org/10.1093/jxb/49.321.693

Lu, X., Liang, E., Wang, Y., Babst, F., Leavitt, S. W., & Julio Camarero, J. (2019). Past the climate optimum: Recruitment is declining at the world's highest juniper shrublines on the Tibetan Plateau. *Ecology*, *100*(2): 1–9. https://doi.org/10.1002/ecy.2557

Markó, G. , Ónodi, G. , Kertész, M. and Altbäcker, V. (2011), Rabbit Grazing as the Major Source of Intercanopy Heterogeneity in a Juniper Shrubland. *Arid Land Research and Management*, 25(2), 176 - 193. http://dx.doi.org/10.1080/15324982.2011.554958

Meehl, G. A., Stocker, T. F., Collins, W. D., Friedlingstein, P., Gaye, A. T., Gregory, J. M., Kitoh, A., Knutti, R., Murphy, J. M.,… & Zhao, Z.-C. (2007). Global Climate Projections. In *Climate Change 2007: The Physical Science Basis. Contribution of Working Group I to the Fourth Assessment Report of the Intergovernmental Panel on Climate Change*. Cambridge University Press, Cambridge, United Kingdom and New York, NY, USA.

Meireles, C., Mendes, P., Vila-Viçosa, C., Cano-Carmona, E., & Pinto-Gomes, C. (2013). Geobotanical aspects of Cytisus oromediterraneus and Genista cinerascens in Serra da Estrela (Portugal). *Plant Sociology*, *50*(1): 23–31. https://doi.org/10.7338/pls2013501/03

Meireles, C., Neiva, R., Passos, I., Vila-Viçosa, C., Paiva-Ferreira, R., & Pinto-Gomes, C. (2009). The management and preservation of communitarian interest habitats in the Natural Park of Serra da Estrela (Portugal). *Acta Botanica Gallica*, *156*(1): 79–88. https://doi.org/10.1080/12538078.2009.10516143

Midolo, G., De Frenne, P., Hölzel, N., & Wellstein, C. (2019). Global patterns of intraspecific leaf trait responses to elevation. *Global Change Biology*, *25*(7): 2485–2498. https://doi.org/10.1111/gcb.14646

Mora, C. (2010). A synthetic map of the climatopes of the serra da estrela (portugal). *Journal of Maps*, *6*(January): 591–608. https://doi.org/10.4113/jom.2010.1112

Myers-Smith, I. H., Hallinger, M., Blok, D., Sass-Klaassen, U., Rayback, S. A., Weijers, S., Trant, A. J., Tape, K. D., Naito, A. T.,…& Wilmking, M. (2015). Methods for measuring arctic and alpine shrub growth: A review. *Earth-Science Reviews*, *140*: 1–13.

https://doi.org/10.1016/j.earscirev.2014.10.004

Ogasa, M., Miki, N. H., Murakami, Y., & Yoshikawa, K. (2013). Recovery performance in xylem hydraulic conductivity is correlated with cavitation resistance for temperate deciduous tree species. *Tree Physiology*, *33*(4): 335–344. https://doi.org/10.1093/treephys/tpt010

Olano, J. M., Almería, I., Eugenio, M., & von Arx, G. (2013). Under pressure: How a Mediterranean high-mountain forb coordinates growth and hydraulic xylem anatomy in response to temperature and water constraints. *Functional Ecology*, *27*(6): 1295–1303. https://doi.org/10.1111/1365-2435.12144

Olano, J. M., Arzac, A., García-Cervigón, A. I., von Arx, G., & Rozas, V. (2013). New star on the stage: Amount of ray parenchyma in tree rings shows a link to climate. *New Phytologist*, *198*(2): 486–495. https://doi.org/10.1111/nph.12113

Olson, M. E., Anfodillo, T., Rosell, J. A., Petit, G., Crivellaro, A., Isnard, S., León-Gómez, C., Alvarado-Cárdenas, L. O., & Castorena, M. (2014). Universal hydraulics of the flowering plants: Vessel diameter scales with stem length across angiosperm lineages, habits and climates. *Ecology Letters*, *17*(8): 988–997. https://doi.org/10.1111/ele.12302

Olson, M. E., Soriano, D., Rosell, J. A., Anfodillo, T., Donoghue, M. J., Edwards, E. J., León-Gómez, C., Dawson, T., Camarero,J. J.,… & Méndez-Alonzo, R. (2018). Plant height and hydraulic vulnerability to drought and cold. *Proceedings of the National Academy of Sciences of the United States of America*, *115*(29): 7551–7556. https://doi.org/10.1073/pnas.1721728115

Pauli, H., Gottfried, M., Dullinger, S., Abdaladze, O., Akhalkatsi, M., Alonso, J. L. B., Coldea, G., Dick, J., Erschbamer, B.,…& Grabherr, G. (2012). Recent plant diversity changes on Europe's mountain summits. *Science*, *336*(6079): 353–355. https://doi.org/10.1126/science.1219033

Peña-Gallardo, M., Vicente-Serrano, S. M., Camarero, J. J., Gazol, A., Sánchez-Salguero, R., Domínguez-Castro, F., El Kenawy, A., Beguería-Portugés, S., Gutiérrez, E., …& Galván, J. D. (2018). Drought sensitiveness on forest growth in peninsular Spain and the Balearic Islands. *Forests*, *9*(9): 524. https://doi.org/10.3390/f9090524

Pittermann, J., & Sperry, J. (2003). Tracheid diameter is the key trait determining the extent of freezing-induced embolism in conifers. *Tree Physiology*, *23*(13): 907–914. https://doi.org/10.1093/treephys/23.13.907

Ren, P., Rossi, S., Camarero, J. J., Ellison, A. M., Liang, E., & Peñuelas, J. (2018). Critical

temperature and precipitation thresholds for the onset of xylogenesis of *Juniperus przewalskii* in a semi-arid area of the north-eastern Tibetan Plateau. *Annals of Botany*, *121*(4): 617–624. https://doi.org/10.1093/aob/mcx188

Rivas-Martinez, S. & Rivas-Saenz, S. Worldwide Bioclimatic Classification System, 1996-2020, Phytosociological Research Center, Spain. http://www.globalbioclimatics.org

Rodriguez-Zaccaro, F. D., Valdovinos-Ayala, J., Percolla, M. I., Venturas, M. D., Pratt, R. B., & Jacobsen, A. L. (2019). Wood structure and function change with maturity: Age of the vascular cambium is associated with xylem changes in current-year growth. *Plant Cell and Environment*, *42*(6): 1816–1831. https://doi.org/10.1111/pce.13528

Rustad, L. E., Campbell, J. L., Marion, G. M., Norby, R. J., Mitchell, M. J., Hartley, A. E., Cornelissen, J. H. C., Gurevitch, J., Alward, R., …& Wright, R. (2001). A meta-analysis of the response of soil respiration, net nitrogen mineralization, and aboveground plant growth to experimental ecosystem warming. *Oecologia*, *126*(4): 543–562. https://doi.org/10.1007/s004420000544

Scholz, A., Klepsch, M., Karimi, Z., & Jansen, S. (2013). How to quantify conduits in wood? *Frontiers in Plant Science*, *4*(March): 1–11. https://doi.org/10.3389/fpls.2013.00056

Schweingruber, F. H., Börner, A., & Schulze, E.-D. (2013). Atlas of Stem Anatomy in Herbs, Shrubs and Trees. *Atlas of Stem Anatomy in Herbs, Shrubs and Trees*. https://doi.org/10.1007/978-3-642-20435-7

Sperry, J. S., & Hacke, U. G. (2004). Analysis of circular bordered pit function I. Angiosperm vessels with homogenous pit membranes. *American Journal of Botany*, *91*(3): 369–385. https://doi.org/10.3732/ajb.91.3.369

Sperry, J. S., Hacke, U. G., & Pittermann, J. (2006). Size and function in conifer tracheids and angiosperm vessels. *American Journal of Botany*, *93*(10): 1490–1500. https://doi.org/10.3732/ajb.93.10.1490

Sperry, J. S., Hacke, U. G., & Wheeler, J. K. (2005). Comparative analysis of end wall resistivity in xylem conduits. *Plant, Cell and Environment* 28: 456–465. https://doi.org/10.1111/j.1365-3040.2005.01287.x

Sperry, J. S., & Sullivan, J. E. M. (1992). Xylem embolism in response to freeze-thaw cycles and water stress in ring-porous, diffuse-porous, and conifer species. *Plant Physiology*, *100*(2): 605–613. https://doi.org/10.1104/pp.100.2.605

Sturm, M. (2005). Changing snow and shrub conditions affect albedo with global

implications. *Journal of Geophysical Research*, *110*(G1): 1–13. https://doi.org/10.1029/2005jg000013

Theurillat, J. P., & Guisan, A. (2001). Potential impact of climate change on vegetation in the European alps: A review. *Climatic Change*, *50*(1–2): 77–109. https://doi.org/10.1023/A:1010632015572

Thomas, P.A., El-Barghathi, M., & Polwart, A. (2007). Biological Flora of the British Isles: Juniperus communis L. Journal of Ecology, 95(6), 1404–1440. https://doi.org/10.1111/j.1365-2745.2007.01308.x

Thuiller, W., Lavorel, S., Araújo, M. B., Sykes, M. T., & Prentice, I. C. (2005). Climate change threats to plant diversity in Europe. *Proceedings of the National Academy of Sciences of the United States of America*, *102*(23): 8245–8250. https://doi.org/10.1073/pnas.0409902102

Tyree, M. T. (1997). The Cohesion-Tension theory of sap ascent: current controversies. *Journal of Experimental Botany*, *48*(10): 1753–1765. https://doi.org/10.1093/jxb/48.10.1753

UWICER (2017). Dendrochronology Manual. Ugyen Wangchuck Institute for Conservation and Environmental Research, Department of Forests and Park Services. UWICER Press, Lamai Goempa, Bumthang, Bhutan

Vaganov, E. A., Hughes, M. K, & Shashkin, A. V. (2008). Growth Dynamics of Conifer Tree Rings: Images of Past and Future Environments . Ecological Studies, Volume 183. Berlin (Germany) and New York: Springer-Verlag. https://doi.org/10.1086/586955

Van Der Knaap, W. O., & Van Leeuwen, J. F. N. (1997). Late Glacial and early Holocene vegetation succession, altitudinal vegetation zonation, and climatic change in the Serra da Estrela, Portugal. *Review of Palaeobotany and Palynology,* 97(1997): 239-285 https://doi.org/10.1016/S0034-6667(97)00008-0

Vieira, J., Campelo, F., & Nabais, C. (2010). Intra-annual density fluctuations of Pinus pinaster are a record of climatic changes in the western Mediterranean region. *Can. J. For. Res*., 40: 1567–1575. https://doi.org/10.1139/X10-096

Vieira, J., Rossi, S., Campelo, F., Freitas, H., & Nabais, C. (2014). Xylogenesis of Pinus pinaster under a Mediterranean climate. *Annals of Forest Science*, *71*(1): 71–80. https://doi.org/10.1007/s13595-013-0341-5

Vieira, J., Rossi, S., Campelo, F., & Nabais, C. (2014). Are neighboring trees in tune? Wood

formation in Pinus pinaster. *European Journal of Forest Research*, *133*(1): 41–50. https://doi.org/10.1007/s10342-013-0734-x

Vieira, J., Campelo, F., Rossi, S., Carvalho, A., Freitasm H., & Nabais, C. (2015) Adjustment Capacity of Maritime Pine Cambial Activity in Drought-Prone Environments. *PLoS ONE* 10(5): e0126223. doi:10.1371/journal.pone.0126223

Vieira, J., Carvalho, A. & Campelo, F. (2020) Tree Growth Under Climate Change: Evidence From Xylogenesis Timings and Kinetics. *Front. Plant Sci.* 11:90. doi: 10.3389/fpls.2020.00090

Wheeler, E.; Baas, P.; Gasson, P. E. (1989). IAWA List of Microscopic Features for Hardwood Identification. IAWA Bull. n. ser. 10 (3), 1989. *Feddes Repertorium*, *101*(11–12), 600–600. https://doi.org/10.1002/fedr.19901011106

Yin, J., & Bauerle, T. L. (2017). A global analysis of plant recovery performance from water stress. *Oikos*, *126*(10): 1377–1388. https://doi.org/10.1111/oik.04534

Zeng, Q., Rossi, S., & Yang, B. (2018). Effects of age and size on xylem phenology in two conifers of northwestern China. *Frontiers in Plant Science*, *8*(January): 1–9. https://doi.org/10.3389/fpls.2017.02264

Zimowski, M., Leuschner, H. H., Gärtner, H., & Bergmeier, E. (2014). Age and diversity of Mediterranean dwarf shrublands: A dendrochronological approach along an altitudinal gradient on Crete. *Journal of Vegetation Science*, *25*(1), 122–134. https://doi.org/10.1111/jvs.12067

Zweifel, R., Rigling, A., & Dobbertin, M. (2009). Species-specific stomatal response of trees to drought - A link to vegetation dynamics? *Journal of Vegetation Science*, *20*(3), 442–454. https://doi.org/10.1111/j.1654-1103.2009.05701.x

APPENDIX I

Table A1. Results of ANOVA analysis for significant differences in shrub size.

Size

ANOVA summary					
	Df	Sum Sq	Mean Sq	F value	Pr(>F)
species	1	18.509	18.509	45.770	3.15e-08
site:species	2	2.149	1.075	2.658	0.0819
Residuals	42	16.984	0.404		
Species					
	diff		lwr	upr	p adj
J-C	1.241925		0.8714646	1.612385	0
Site:Species					
	diff		lwr	upr	p adj
NSA:J-NSA:C	1.78910455		0.83993461	2.7382745	0.0000194
PEG:J-NSA:C	1.19627968		0.24710974	2.1454496	0.0064072
COB:J-NSA:C	1.03299742		0.08382748	1.9821674	0.0258815
NSA:J-PEG:C	1.77123138		0.82206145	2.7204013	0.0000233
PEG:J-PEG:C	1.17840651		0.22923657	2.1275764	0.0075123
COB:J-PEG:C	1.01512425		0.06595431	1.9642942	0.0298930
NSA:J-COB:C	1.51437035		0.56520041	2.4635403	0.0003133

Table A2. Results of ANOVA analysis for significant differences in shrub age.

Age

ANOVA summary					
	Df	Sum Sq	Mean Sq	F value	Pr(>F)
site	2	2.057	1.029	5.207	0.00955
species	1	5.360	5.360	27.130	5.39e-06
site:species	2	9.842	4.921	24.906	7.37e-08
Residuals	42	8.298	0.198		
Site					
	diff		lwr	upr	p adj
PEG-NSA	0.5022212		0.1204152	0.88402717	0.0073163
Species					
	diff		lwr	upr	p adj
J-C	0.6683539		0.4094014	0.9273063	5.4e-06
Site:Species					
PEG:J-NSA:C	1.6844123		1.02094052	2.3478841	0.0000000
COB:C-PEG:C	0.7896167		0.12614492	1.4530885	0.0115117
NSA:J-PEG:C	0.6799699		0.01649810	1.3434417	0.0417288
PEG:J-PEG:C	1.8441133		1.18064152	2.5075851	0.0000000
PEG:J-COB:C	1.0544966		0.39102482	1.7179684	0.0003318
PEG:J-NSA:J	1.1641434		0.50067164	1.8276152	0.0000687
COB:J-PEG:J	-1.4138171		-2.07728892	-0.7503454	0.0000017

Table A3. Results of correlation analysis between shrub ring width and shrub age.

```
        Pearson's product-moment correlation

data:  log(data$SRW) and log(data$age)
t = -9.6978, df = 46, p-value = 1.07e-12
alternative hypothesis: true correlation is not equal to 0
95 percent confidence interval:
 -0.8951764 -0.6978236
sample estimates:
      cor
-0.819476
```

Table A4. Results of ANOVA analysis for significant differences in shrub ring.

SRW				
ANOVA summary				
	Df	Sum Sq	Mean Sq	F value	Pr(>F)
species	1	3.659	3.659	22.695	2.28e-05
site:species	2	3.805	1.903	11.801	8.57e-05
Residuals	42	6.771	0.161		
Species				
		diff	lwr	upr	p adj
J-C		-0.5521835	-0.786098	-0.318269	2.28e-05
Site:Species				
		diff	lwr	upr	p adj
PEG:J-NSA:C		-0.89132182	-1.49064289	-0.29200075	0.0008576
COB:C-PEG:C		-0.76261342	-1.36193449	-0.16329235	0.0057793
NSA:J-PEG:C		-0.79445394	-1.39377501	-0.19513287	0.0036540
PEG:J-PEG:C		-1.31417421	-1.91349528	-0.71485314	0.0000009
COB:J-PEG:C		-0.73338810	-1.33270917	-0.13406703	0.0087213

Table A5. Results of t-test analysis of SRW temporal growth by site and species. Significant values are highlighted. SRW - Shrub Ring Width

SRW								
Year	J	C	NSAJ	PEGJ	COBJ	NSAC	PEGC	COBC
2019	1.21E-07	0.00012	0.8000	0.0008	0.0002	0.0663	0.0010	0.2618
2018	5.91E-09	0.00076	0.0048	0.0225	0.0020	0.0017	0.0191	0.5990
2017	9.19E-11	2.45E-06	0.0041	0.0028	0.0004	0.0146	0.0004	0.1268
2016	2.53E-07	5.25E-05	0.0011	0.1283	0.0114	0.0253	0.0076	0.2317
2015	8.51E-11	1.04E-06	0.0001	0.0048	0.0003	0.0024	0.0013	0.1346

Table A6. Results of ANOVA analysis for significant differences in branch age

Branch age

ANOVA summary

	Df	Sum Sq	Mean Sq	F value	Pr(>F)
site	2	6.429	3.214	30.30	9.33e-12 ***
species	1	6.092	6.092	57.43	3.53e-12 ***
site:species	2	9.977	4.989	47.02	< 2e-16 ***
Residuals	148	15.700	0.106		

Site

	diff	lwr	upr	p adj
PEG-NSA	0.4946008	0.34358888	0.6456127	0.0000000
COB-NSA	0.2537006	0.09109643	0.4163047	0.0009006
COB-PEG	-0.2409002	-0.38995399	-0.0918464	0.0005582

Species

	diff	lwr	upr	p adj
J-C	0.4102214	0.3019795	0.5184633	0

Site:Species

	diff	lwr	upr	p adj
PEG:C-NSA:C	0.3240860	0.000959474	0.64721255	0.0488561
COB:C-NSA:C	0.8886393	0.576563095	1.20071548	0.0000000
NSA:J-NSA:C	0.7076773	0.412952428	1.00240211	0.0000000
PEG:J-NSA:C	1.1878841	0.914932006	1.46083609	0.0000000
COB:J-NSA:C	0.5489778	0.247891265	0.85006435	0.0000072
COB:C-PEG:C	0.5645533	0.262477555	0.86662899	0.0000039
NSA:J-PEG:C	0.3835913	0.099476979	0.66770554	0.0019985
PEG:J-PEG:C	0.8637980	0.602338654	1.12525742	0.0000000
PEG:J-COB:C	0.2992448	0.051571999	0.54691753	0.0082497
COB:J-COB:C	-0.3396615	-0.618035482	-0.06128747	0.0073633
PEG:J-NSA:J	0.4802068	0.254789428	0.70562413	0.0000001
COB:J-PEG:J	-0.6389062	-0.872579851	-0.40523263	0.0000000

Table A7. Results of ANOVA analysis for significant differences in average lumen area

ALA

ANOVA summary

	Df	Sum Sq	Mean Sq	F value	Pr(>F)
site	2	1.06	0.5277	2.467	0.0883
species	1	0.76	0.7566	3.537	0.0620
site:species	2	0.52	0.2582	1.20	0.3021
Residuals	148	31.66	0.2139		

Table A8. Results of ANOVA analysis for significant differences in maximum lumen area

MLA

ANOVA summary

	Df	Sum Sq	Mean Sq	F value	Pr(>F)
site	2	7.38	3.69	14.398	1.93e-06
species	1	53.15	53.15	207.291	< 2e-16
site:species	2	1.44	0.72	2.818	0.0629
Residuals	148	37.95	0.26		

Site

	diff	lwr	upr	p adj
NSA-COB	-0.46115093	-0.7139398	-0.208362	0.0000845
PEG-COB	-0.48912918	-0.7208523	-0.257406	0.0000048

Species

	diff	lwr	upr	p adj
J-C	-1.211637	-1.37991 3	-1.043361	0

Site:Species

	diff	lwr	upr	p adj
NSA:C-COB:C	-0.65244204	-1.1376043	-0.1672798	0.0021134
COB:J-COB:C	-1.46344848	-1.8962164	-1.0306806	0.0000000
NSA:J-COB:C	-1.60168127	-2.0237325	-1.1796300	0.0000000
PEG:J-COB:C	-1.64258250	-2.0276214	-1.2575436	0.0000000
COB:J-NSA:C	-0.81100643	-1.2790839	-0.3429290	0.0000231
NSA:J-NSA:C	-0.94923922	-1.4074266	-0.4910518	0.0000002
PEG:J-NSA:C	-0.99014046	-1.4144792	-0.5658017	0.0000000
COB:J-PEG:C	-1.09411357	-1.5460567	-0.6421705	0.0000000
NSA:J-PEG:C	-1.23234636	-1.6740383	-0.7906545	0.0000000
PEG:J-PEG:C	-1.27324759	-1.6797196	-0.8667756	0.0000000

Table A9. Results of ANOVA analysis for significant differences in maximum lumen area

K_H

ANOVA summary					
	Df	Sum Sq	Mean Sq	F value	Pr(>F)
site	2	107.0	53.50	9.694	0.000111
species	1	96.4	96.40	17.467	4.98e-05
Residuals	148	816.8	5.52		
Site					
	diff	lwr	upr	p adj	
PEG-COB	-1.9815061	-3.056587	-0.90642469	0.0000706	
PEG-NSA	-1.0756308	-2.164835	0.01357378	0.0537366	
Species					
	diff	lwr	upr	p adj	
J-C	-1.631787	-2.412504	-0.8510701	6.03e-05	
Site:Species					
	diff	lwr	upr	p adj	
NSA:J-COB:C	-2.0899733	-4.048083	-0.1318633	0.0290296	
PEG:J-COB:C	-3.0696162	-4.856007	-1.2832251	0.0000277	
PEG:J-NSA:C	-2.9121518	-4.880875	-0.9434287	0.0004891	
PEG:J-PEG:C	-2.1573072	-4.043137	-0.2714773	0.0149336	
PEG:J-COB:J	-2.1839000	-3.869319	-0.4984807	0.0034988	

Table A10. Results of ANOVA analysis for significant differences in BRW. BRW – Branch Ring Width

BRW

ANOVA summary

	Df	Sum Sq	Mean Sq	F value	Pr(>F)
site	2	5.25	2.6239	7.498	0.000791
species	1	1.76	1.7576	5.023	0.026507
site:species	2	3.49	1.7436	4.983	0.008050
Residuals	148	51.79	0.3499		

Tukey posthoc

Site

	diff	lwr	upr	p adj
PEG-NSA	-0.3653506	-0.6396262	-0.0910750	0.0055127
COB-NSA	0.0175552	-0.2777748	0.3128852	0.9891413
COB-PEG	0.3829058	0.1121866	0.6536250	0.0029435

Species

	diff	lwr	upr	p adj
Juniperus-Cytisus	0.2203419	0.0237473	0.4169364	0.0283004

Site:Species

	diff	lwr	upr	p adj
PEG:Cytisus-NSA:Cytisus	-0.356863338	-0.9437424	0.23001577	0.4975126
COB:Cytisus-NSA:Cytisus	-0.344733564	-0.9115425	0.22207534	0.4972664
NSA:Juniperus-NSA:Cytisus	0.009581885	-0.5257126	0.54487637	0.9999999
PEG:Juniperus-NSA:Cytisus	-0.360188136	-0.8559377	0.13556147	0.2941211
COB:Juniperus-NSA:Cytisus	0.333097273	-0.2137517	0.87994621	0.4955390
COB:Cytisus-PEG:Cytisus	0.012129775	-0.5365157	0.56077530	0.9999998
NSA:Juniperus-PEG:Cytisus	0.366445224	-0.1495778	0.88246825	0.3192849
PEG:Juniperus-PEG:Cytisus	-0.003324798	-0.4782008	0.47155124	1.0000000
COB:Juniperus-PEG:Cytisus	0.689960611	0.1619612	1.21795999	0.0031297
NSA:Juniperus-COB:Cytisus	0.354315449	-0.1387616	0.84739253	0.3061934
PEG:Juniperus-COB:Cytisus	-0.015454572	-0.4652906	0.43438150	0.9999986
COB:Juniperus-COB:Cytisus	0.677830836	0.1722336	1.18342808	0.0022066
PEG:Juniperus-NSA:Juniperus	-0.369770021	-0.7791847	0.03964462	0.1017884
COB:Juniperus-NSA:Juniperus	0.323515387	-0.1464808	0.79351159	0.3544339
COB:Juniperus-PEG:Juniperus	0.693285408	0.2688753	1.11769549	0.0000796